Neurotoxicity Research (2019) 36:472–490
https://doi.org/10.1007/s12640-019-00064-4

ORIGINAL ARTICLE

The Long-Term Impairment in Redox Homeostasis Observed in the Hippocampus of Rats Subjected to Global Perinatal Asphyxia (PA) Implies Changes in Glutathione-Dependent Antioxidant Enzymes and TIGAR-Dependent Shift Towards the Pentose Phosphate Pathways: Effect of Nicotinamide

C. Lespay-Rebolledo[1] · A. Tapia-Bustos[1] · D. Bustamante[1] · P. Morales[1,2] · M. Herrera-Marschitz[1]

Received: 14 March 2019 / Revised: 8 May 2019 / Accepted: 9 May 2019 / Published online: 11 June 2019

Abstract

We have recently reported that global perinatal asphyxia (PA) induces a regionally sustained increase in oxidized glutathione (GSSG) levels and GSSG/GSH ratio, a decrease in tissue-reducing capacity, a decrease in catalase activity, and an increase in apoptotic caspase-3-dependent cell death in rat neonatal brain up to 14 postnatal days, indicating a long-term impairment in redox homeostasis. In the present study, we evaluated whether the increase in GSSG/GSH ratio observed in hippocampus involves changes in glutathione reductase (GR) and glutathione peroxidase (GPx) activity, the enzymes reducing glutathione disulfide (GSSG) and hydroperoxides, respectively, as well as catalase, the enzyme protecting against peroxidation. The study also evaluated whether there is a shift in the metabolism towards the penthose phosphate pathway (PPP), by measuring TIGAR, the TP53-inducible glycolysis and apoptosis regulator, associated with delayed cell death, further monitoring calpain activity, involved in *bax*-dependent cell death, and XRCC1, a scaffolding protein interacting with genome sentinel proteins. Global PA was induced by immersing fetus-containing uterine horns removed by a cesarean section from *on term* rat dams into a water bath at 37 °C for 21 min. Asphyxia-exposed and sibling cesarean-delivered fetuses were manually resuscitated and nurtured by surrogate dams. Animals were euthanized at postnatal (P) days 1 or 14, dissecting samples from hippocampus to be assayed for glutathione, GR, GPx (all by spectrophotometry), catalase (Western blots and ELISA), TIGAR (Western blots), calpain (fluorescence), and XRCC1 (Western blots). One hour after delivery, asphyxia-exposed and control neonates were injected with either 100 μl saline or 0.8 mmol/kg nicotinamide, i.p., shown to protect from the short- and long-term consequences of PA. It was found that global PA produced (i) a sustained increase of GSSG levels and GSSG/GSH ratio at P1 and P14; (ii) a decrease of GR, GPx, and catalase activity at P1 and P14; (iii) a decrease at P1, followed by an increase at P14 of TIGAR levels; (iv) an increase of calpain activity at P14; and (v) an increase of XRCC1 levels, but only at P1. (vi) Nicotinamide prevented the effect of PA on GSSG levels and GSSG/GSH ratio, and on GR, GPx, and catalase activity, also on increased TIGAR levels and calpain activity observed at P14. The present study demonstrates that the long-term impaired redox homeostasis observed in the hippocampus of rats subjected to global PA implies changes in GR, GPx, and catalase, and a shift towards PPP, as indicated by an increase of TIGAR levels at P14.

All authors declare no conflict of interest on any section of the manuscript.

✉ P. Morales
pmorales@med.uchile.cl

✉ M. Herrera-Marschitz
mh-marschitz@med.uchile.cl; mhmarschitz@gmail.com

C. Lespay-Rebolledo
carolynelespay@gmail.com

A. Tapia-Bustos
ac.tapiabustos@gmail.com

D. Bustamante
dbustama@med.uchile.cl

[1] Programme of Molecular & Clinical Pharmacology, ICBM, Medical Faculty, University of Chile, Av. Independencia, 1027 Santiago, Chile

[2] Department of Neuroscience, Medical Faculty, University of Chile, Av. Independencia, 1027 Santiago, Chile

Keywords Pentose phosphate pathway · TIGAR · Glutathione reductase · Glutathione peroxidase · Catalase · Neonatal hippocampus · Perinatal asphyxia · XRCC1 · Calpain · Delayed cell death · Rat

Abbreviations

Ac-LLY-AFC	Ac-Leu-Leu-Tyr-7-amino-4-trifluoromethylcoumarin
AFC	7-amino-4-trifluoromethylcoumarin
AIF	Apoptosis inducing factor
AS	Asphyxia-exposed rats
a.u.	Arbitrary units
Bax	Bcl-2 associated X protein apoptosis regulator
Bid	BH3 interacting domain death agonist
BCA	Bicinchoninic acid
BSA	Bovine serum albumin
C	Cerebellum
CS	Control saline rats
DTNB	5, 5′-Dithio-bis-[2-nitrobenzoic acid]
DTT	Dithiothreitol
ΔA	Changes in absorbance per minute
EDTA	Ethylenediaminetetraacetic acid
EGTA	Ethylene glycol-bis (β-aminoethylether)-N, N, N′, N′-tetraacetic acid
ELISA	Enzyme-linked immunosorbent assay
GPx	Glutathione peroxidase
GR	Glutathione reductase
GSH	Reduced glutathione
GSSG	Oxidized glutathione
G22	Gestation day 22
HI	Hypoxic-ischemic
HIE	Hypoxic-ischemia encephalopathy
HRP	Horseradish peroxidase
H_2O_2	Hydrogen peroxide
H2Od	Distillated water
HK2	Hexokinase 2
i.p	Intraperitoneal injection
IgG (H + L)	Immunoglobulin type G (Heavy + Light chains)
mU/mL	Milliunits enzymatic per milliliter
NaCl	Sodium chloride
NAD^+	Oxidized nicotinamide adenine dinucleotide
NADH	Reduced nicotinamide adenine dinucleotide
$NADP^+$	Oxidized β-Nicotinamide adenine dinucleotide 2′-phosphate
NADPH	Reduced β-Nicotinamide adenine dinucleotide 2′-phosphate
NADK	NAD+ kinase
NaF	Sodium fluoride
NAMPT	Nicotinamide phosphoribosyltransferase
Nico	Nicotinamide
NMNAT	Nicotinamide mononucleotide adenyltransferase
NMN	Nicotinamide mononucleotide
PA	Perinatal asphyxia
PARP1	Poly(ADP-ribose) polymerase 1
PBS	Phosphate buffer saline
PK	Pyruvate kinase
PMSF	Phenylmethylsulfonyl fluoride
PFK1	Phosphofructokinase 1
PPP	Pentose phosphate pathway
P	Postnatal day
TP53	Tumor protein p53
p53	Cellular tumor antigen p53
RE	Reticulum endoplasmic
RIPA	Radio-immune precipitation assay buffer
ROS	Reactive oxygen species
R5P	Ribulose-5-phosphate
SEM	Standard error of the means
SOD	Superoxide dismutase
SDS	Sodium dodecyl sulfate
SDS-PAGE	Sodium dodecyl sulfate polyacrylamide gel
SSBR	Single-strand break DNA
TIGAR	TP53-induced glycolysis and apoptosis regulator
Tris-HCl	Tris(hydroxymethyl)aminoethane-chloride acid buffer
TBST	Tris-buffered saline containing 0.1% Tween-20
TNF-alpha	Tumor necrosis factor alpha
U/ml	Units enzymatic per milliliter
Veh	Vehicle
WB	Western blots
XIAP	X-linked inhibitor of apoptosis protein
XRCC1	X-ray repair cross-complementing protein 1

Introduction

Interruption of oxygen viability, as result of impaired placental gas exchange at labor or delay/interruption of autonomous pulmonary respiration at delivery, is a clinical condition known as perinatal asphyxia (PA) (see Herrera-Marschitz et al. 2011). PA may result in fetal demise, neonatal death, or long-term neurological deficits affecting neonate's survivors. The brain damage induced by PA is known as hypoxic-ischemic encephalopathy (HIE) and is a major cause

of mortality and morbidity in neonates. The severity and neurological manifestations of HIE depend upon the duration of the hypoxic insult and the age of the affected fetus/baby, resulting in a different profile of brain damage, affecting brainstem and mesencephalic nuclei, basal ganglia, and/or cortical areas, including hippocampus (Swarte et al. 2009).

Several molecular defenses are activated immediately, during and/or after the re-oxygenation period, making survival possible, but also impairing brain development, or even worse, inducing brain damage, days, weeks, or months after birth, consolidating the neurological dysfunction observed in PA-exposed neonates (see Fleiss and Gressens 2012; Hassell et al. 2015; Hagberg et al. 2016). The energetic deficit induced by oxygen deprivation and the oxidative stress produced by the compulsory re-oxygenation alters brain metabolism, triggering a cascade of events affecting recovery and brain development. Several molecular events can be listed, including glutamate- and Ca^{+2} -homeostasis, excitotoxicity, mitochondrial failure, generation of free radicals and oxidative species, and pro-inflammatory molecules (see Blomgren and Hagberg 2005; Liu and McCullough 2013; Herrera-Marschitz et al. 2018; Leaw et al. 2017). These cascades will affect brain regions differently, depending upon their energetic requirements and developmental stages, making especially vulnerable regions at a spur of development when the metabolic insult occurs, defining windows of vulnerability for different brain regions (see Marriott et al. 2017), the hippocampus shown to be a particularly vulnerable region at neonatal stages (Morales et al. 2005, 2008, 2010).

We have recently reported that global PA affects rat neonatal brain, inducing a sustained oxidative stress, reflected by an increase of oxidized glutathione (GSSG) levels and GSSG/GSH ratio; together with a decrease in tissue-reducing capacity, and catalase activity, resulting in apoptotic caspase-3-dependent cell death, mainly in mesencephalon and hippocampus, indicating a long-term, region specific, impairment in redox homeostasis (Lespay-Rebolledo et al. 2018).

In the present study, we investigated whether the sustained oxidative stress in hippocampus observed after PA implies regulation of antioxidant enzymes and NAD^+ and $NADP^+$ viability, since the antioxidant machinery is promoted by the thioredoxin/peroxiredoxin and glutathione systems, sustained by nicotinamide adenine dinucleotide phosphate (NADPH), which is yielded by the shunt of glucose-6-phosphate to the pentose phosphate pathway (PPP), whose flux is enhanced by the TP53-induced glycolysis and apoptosis regulator (TIGAR) (Bensaad et al. 2006). The PPP generates NADPH and ribose 5-phosphates (R5P), required for nucleotide synthesis, DNA repair, cell proliferation, and growth (Bensaad et al. 2006). NADPH is also required for GSH generation, and for providing energy preserving mitochondrial function, via glutathione reductase (GR). Furthermore, GSH is the electron donor for reduction of detrimental peroxides by glutathione peroxidase (GPx), in synergy with catalase (Dringen and Hamprecht 1997, Dringen 2000; see Stincone et al. 2015). Thus, we have investigated the effect of PA on glutathione, GR, GPx, catalase, and TIGAR levels evaluated at postnatal days 1 and 14, a critical period for brain rat development.

Global PA leads to apoptotic-like cell death, with a region-dependent time course (Morales et al. 2005, 2008). In hippocampus, nuclear Hoechst staining positive apoptosis has been observed up to 1 month after delivery in PA-exposed animals (Morales et al. 2008), while increase in cleaved caspase-3 has only been observed at P1 and P7 in PA-exposed rat neonates (Lespay-Rebolledo et al. 2018), suggesting that a caspase-3-independent-delayed cell death can also occur. Thus, we have evaluated here the effect of PA on calpain activity, shown to play a synergism with caspase-3 (Blomgren et al. 2001), also associated to caspase-3 independent, but bax-dependent, excitotoxic neuronal injury (D'Orsi et al. 2012).

Suppression and/or overactivation of gene expression have been shown to occur immediately or during the re-oxygenation period following PA (Labudova et al. 1999; Seidl et al. 2000; Mosgoeller et al. 2000; Lubec et al. 2002), associated to overexpression of a number of sentinel proteins whenever the integrity of the genome is compromised (see Herrera-Marschitz et al. 2011), including X-ray repair cross-complementing protein 1 (XRCC1), a scaffolding protein interacting with sentinel proteins, such as poly(ADP-ribose) polymerase-1 (PARP-1), for repairing base-excision (Chiappe-Gutierrez et al. 1998; see London 2015). PARP-1 has been shown to be significantly increased during the first hours following PA (Neira-Peña et al. 2014, 2015), an effect prevented by nicotinamide (Allende-Castro et al. 2012; Neira-Peña et al. 2015) and selective siRNA knockdown of PARP-1 (Vio et al. 2018). XRCC1 expression has also shown to be increased following PA (Chiappe-Gutierrez et al. 1998), originally described as involved in repairing DNA single-strand breaks produced by exposure to ionizing radiation, shown to interact with DNA ligase III, polymerase β, and PARP-1 (London 2015), also following PA (see Herrera-Marschitz et al. 2014). We have investigated further whether the sustained oxidative stress reported to follow PA involves XRCC1 expression.

A main concern relates to therapeutic strategies against the long-term effects produced by PA, which in the clinical scenario are limited, and mainly based on hypothermia, still waiting for consensus on clinical protocols (Ahearne et al. 2016). The idea of nicotinamide as a therapeutic strategy has been forwarded based on its feature of inhibiting PARP-1 overexpression by an end-of-product enzymatic inhibitory mechanism (see Herrera-Marschitz et al. 2011), although the therapeutic effect of nicotinamide can also be explained by the fact that nicotinamide is a physiological precursor of NAD^+ and $NADP^+$, replenishing ATP, but also GSH stores

(Kawamura et al. 2016; Wang et al. 2016; Zhang et al. 2016). Therefore, nicotinamide has also been evaluated here on the metabolic cascade elicited by PA.

Materials and Methods

Animals

Wistar albino rats from the animal station of the Molecular & Clinical Pharmacology Programme, ICBM, Faculty of Medicine, University of Chile, Santiago, Chile, were used along the experiments. The animals were kept on a temperature- and humidity-controlled environment with a 12/12-h light/dark cycle, and access to water and food ad libitum when not used in the experiments, monitoring permanently the well being of the animals by qualified personnel.

Perinatal Asphyxia

Pregnant Wistar rats within the last day of gestation (G22) were euthanized by neck dislocation and hysterectomized. One or two pups per dam were removed immediately and used as non-asphyxiated cesarean-delivered controls (CS). The remaining fetuses-containing uterine horns were immersed into a water bath at 37 °C for 21 min (asphyxia-exposed rats, AS). Following asphyxia, the uterine horns were incised and the pups removed, stimulated to breathe and, after an approximately 40-min observation period on a warming pad, evaluated with an Apgar scale for rats, according to Dell'Anna et al. (1997), and nurtured by a surrogate dam. The Apgar parameters were continuously monitored up to P14, comparing the same CS and AS cohorts.

Nicotinamide Treatment

One hour after birth, asphyxia-exposed and control rat neonates were divided into six experimental groups: control (CS); control + vehicle (CS Veh); control + nicotinamide (CS Nico); asphyxia (AS); asphyxia + vehicle (AS Veh), and AS + nicotinamide (AS Nico). Nicotinamide was injected intraperitoneally (i.p.) in a single dose of 0.8 mmol/kg (Sigma, St. Louis, MO, USA) (diluted in 0.9% NaCl; in a volume of 0.1 mL/kg body weight, i.p.). The vehicle groups received 0.9% NaCl in a volume of 0.1 mL/kg body weight, i.p.

Tissue Sampling

The animals were euthanized at P1 and P14 by rapid decapitation. The brain was quickly removed for dissecting out the hippocampus. Dissection was performed on ice, using a newborn rat brain slicer (Zivic Instruments Pittsburgh, PA 15237 USA). The samples were stored at − 80 °C pending further experiments.

Homogenization of Hippocampus Tissue for Western Blots

Hippocampus was homogenized in RIPA lysis buffer (50 mM Tris–HCl, pH 7.2, 0.15 M NaCl, 1.0 mM EDTA, 0.1% SDS, 1.0% Triton X-100, 1.0% sodium deoxycholate) supplemented with phosphatase and protease inhibitors (1 mM sodium orthovanadate, 1 mM PMSF, 5 mM EDTA, 1 mM EGTA, 10 mM NaF) and a protease inhibitor cocktail, CALBIOCHEMset III (EMD Biosciences Inc., USA; Merck KGaA, Darmstadt, Germany). Tissue was lysed, by passing it through 21- and then 27-gauge needles, ten times. The lysates were incubated on ice for 20 min and centrifuged at 13,500 rpm, 4 °C, for 20 min. The supernatant was transferred to fresh Eppendorf tubes and stored at − 80 °C pending further experiments.

Homogenization of Hippocampus Tissue for Glutathione and Enzymatic Assays

Hippocampus was homogenized in a phosphate buffer supplemented with a protease inhibitor cocktail (CALBIOCHEM set III, EMD Biosciences Inc., USA; Merck KGaA, Darmstadt, Germany), then lysed by passing it through a 27-gauge needle, ten times on ice and centrifuged at 14,000 rpm, at 4 °C for 10 min. The supernatants were recollected according to the respective assays. Both, glutathione and enzymatic assays, were carried out during the same day (Lespay-Rebolledo et al. 2018).

Quantification of Proteins

The total protein concentration was determined using a commercially available bicinchoninic acid (BCA) assay kit from Pierce (Thermo Fisher Scientific, Rockford, IL USA). Absorbance was measured at 562 nm in a Multi-Mode Microplate Reader (Synergy HT Biotek Instruments, Inc., Winooski, VT, USA).

Glutathione Determination

Sample Preparation The hippocampus was homogenized in 40 μL 0.1 M potassium phosphate buffer with 5 mM EDTA disodium salt, pH 7.5. The recollected supernatant was deproteinated by adding 20 μL of previously cold 5% metaphosphoric acid and 10 μL of 10% trichloroacetic acid. The mixture was kept on ice for 5 min and centrifuged at 5000 rpm, 4 °C, for 5 min. The supernatant was transferred to fresh Eppendorf tubes and used for total GSH and GSSG determination during the same day.

Total GSH Measurement by Recycling Method Twenty microliters of de-proteinated samples was added to a microplate of 96 wells containing 200 μL of incubation buffer (500 μL 20% β-NADPH, 200 μL 6 mM DTNB, and 300 μL H2Od) to allow the oxidation of GSH by DTNB, resulting in the formation of GSSG and TNB. Then, 5 μL of glutathione reductase (266 U/ml, adding baker's yeast *S. cerevisiae* 100–300 units/mg protein, Sigma-Aldrich, Saint Louis, MO, USA) is added to allow the recycling of GSSG to GSH. The absorbance of TNB was measured at 412 nm each 10 s for 1 min in a Multi-Mode Microplate Reader (Synergy HT Biotek Instruments, Inc., Winooski, VT, USA). The rate of TNB formation is directly proportional to the recycling reaction, which is directly proportional to total GSH in samples.

GSSG Measurement by Derivatization Fifty microlitres of de-proteinated samples were mixed with 1 μL [4-vinylpyridine] (1:10 in phosphate buffer) to allow the derivatization of GSH, leaving only GSSG for quantification. The derivatization mixture was vigorously stirred in a vortex and incubated for 1 h under dark at room temperature and stirring. Then, 3 μL triethanolamine (1:100 in phosphate buffer) was added to each sample, mixed vigorously in a vortex and incubated at room temperature for 10 min while stirring, leading to neutralization of excess of [4-vinylpyridine]. Then, 20 μl of the derivatized samples was added to a microplate of 96 wells containing 200 μL of incubation buffer, and 5 μL of glutathione reductase (to reduce GSSG and to allow recycling reaction). The absorbance of TNB was measured at 412 nm each 10 s for 1 min in a Multi-Mode Microplate Reader as above. The rate of formation TNB is directly proportional to the recycling reaction which is directly proportional to GSSG in samples.

Analysis Standard curves were set up for GSH, 5–60 μM and GSSG, 0.25–3.0 μM (Sigma-Aldrich, Saint Louis, MO, USA). The change of absorbance (ΔA412nm) over 1 min was calculated for standard solutions and samples by linear regression (A vs time); the corrected ΔA412 nm was obtained by subtraction of ΔA412 nm blank sample. The corrected ΔA412 nm was used to determine the concentration of total GSH and GSSG by interpolation into respective standard curves (ΔA412 nm vs concentration). Total GSH and GSSG concentration was expressed in micromole per milligram of total protein. The GSH (total GSH-2GSSG) was determined to calculate the GSSG/GSH ratio.

GR Activity

For glutathione reductase (GR), the hippocampus was homogenized in 100 μL 0.2 M potassium phosphate buffer, pH 7.6, supplemented with 2 mM EDTA. Twenty microliters of samples was added to a microplate of 96 wells containing 100 μL of homogenization buffer, 10 μL of 20 mM GSSG, and 10 μL 2 mM NADPH. The absorbance was measured at 340 nm every 15-s intervals for 5 min at 25 °C in a the multi-mode microplate reader (Synergy HT Biotek Instruments, Inc., Winooski, VT, USA). The change in absorbance (ΔA 340 nm) over 5 min was obtained for each sample and interpolated in a calibration curve for GR activity (GR, 5–25 mU/mL; 266 U/ml, adding baker's yeast *S. cerevisiae*, 100–300 units/mg protein, Sigma-Aldrich, Saint Louis, MO, USA). The GR activity in the samples was expressed as mU/mL per microgram of total protein.

GPx Activity

For glutathione peroxidase (GPx), the hippocampus was homogenized in 100 μL 50 mM potassium phosphate buffer, pH 7.4, supplemented with 5 mM EDTA, 100 μL of samples was added to a microplate of 96 wells containing 50 μL of reaction buffer: 20 μL 40 mM β-NADPH (MP Biomedicals LCC, Solon, Ohio, USA), 2 μL GR 5 mU/mL (266 U/ml, adding baker's yeast *S. cerevisiae*, 100–300 units/mg protein, Sigma-Aldrich, Saint Louis, MO, USA), 2 μL 2 mM GSH (Sigma-Aldrich, Saint Louis, MO, USA), and 33 μL homogenization buffer. The plate was incubated for 15 min at room temperature. Thereafter, 100 μL 3% H_2O_2 (Merck KGaA, Darmstadt, Germany) was added. The absorbance was measured at 340 nm every 5-min intervals for 30 min at 25 °C in a Multi-Mode Microplate Reader (Synergy HT Biotek Instruments, Inc., Winooski, VT, USA). The change of absorbance (ΔA 340 nm) over 30 min for each sample was determined and interpolated in the calibration curve for β-NADPH (10–120 nmol). The GPx activity was expressed as nmol β-NADPH/min/mL per microgram of total protein.

Catalase Activity

Catalase activity and protein levels were measured according to the procedure described by Lespay-Rebolledo et al. (2018). Hippocampus samples from animals at P1 and P14 were processed according to the protocol provided by a catalase-specific activity kit (ab118184 Abcam, Cambridge, UK). Each experimental N corresponded to a pool of two hippocampus samples. Both catalase activity and protein levels were detected by luminescence and absorbance, respectively assayed in a multimode microplate reader (Synergy HT Biotek Instruments, Winooski, VT, USA) every 5 min for 30 min. Catalase activity was determined according to the exponential decay of H_2O_2. The rate constant (k), reflecting catalase activity, was determined from the luminescence data according to the equation: $k = \ln(S1/S2)/dt$, where dt is the measured time interval; S1 and S2 are H_2O_2 levels at time t_1 and t_2, respectively. The specific catalase activity was obtained by dividing the rate constant (k) by absorbance values of catalase and total protein, expressed in milligrams.

Calpain Activity Assay

Calpain was measured using a calpain activity kit (MAK228; Sigma-Aldrich, St Louis, MO, USA). Brain samples from animals at P1 and P14 were processed according to the protocol provided by the kit. The calpain activity was quantificated by fluorescence in a Synergy HT equipment (Synergy HT Biotek Instruments, Winooski, VT, USA). The Ac-LLY-AFC is cleaved by calpain releasing AFC which emits a yellow-green fluorescence (max = 505 nm). Calpain activity was obtained by interpolation of fluorescence intensity in a calibration curve for calpain I (0.1–0.8 units), expressed as enzymatic units, and normalized per milligram of total protein present in each sample. The MAK228 kit provides an estimation of total calpain activity, only.

Western Blots for Catalase, TIGAR, and XRCC1

Proteins were separated by electrophoresis onto SDS-PAGE. Gels 4–10% for catalase, 4–12% for TIGAR, and 4–8% for XRCC1 were used for separation of proteins. Samples were mixed with loading buffer (30% glycerol, 6% SDS, 15% DTT, 0.2% bromophenol blue, and 120 mM Tris–HCl buffer pH 6.8) and immediately heated at 95 °C for 5 min. The amount of loaded sample onto the wells was according to the linear range for each protein: 25–35 μg for catalase, 15–35 μg for TIGAR, and 30–40 μg for XRCC1. Gels were run at constant 40 V for the stacking gel and at 80 V for the separating gel. The separated proteins were electroblotted on BioTrace TM pure nitrocellulose membranes (Pall Corporation, Pensacola, FL, USA) at 250 mA, 4 °C; the time of transference was 90 min for catalase, 60 min for TIGAR, and 100 min for XRCC1. A Ponceau red solution was used to visualize transference of proteins onto the membranes, and images were digitalized to estimate total protein, as loading control. Thereafter, Ponceau red was removed with water. The blotted membranes were blocked with 2.5% (XRCC1) or 5% BSA (catalase and TIGAR) dissolved in Tris-buffered saline containing 0.1% Tween-20 (TBST) at room temperature for 1 h. The incubation with primary antibodies was performed at 4 °C overnight. The dilution used for catalase (Rabbit polyclonal, PA5-23246. Thermo Fisher Scientific, Rockford, IL, USA) was 1:500, for TIGAR (Rabbit polyclonal, PA5-20346; Thermo Fisher Scientific, Rockford, IL, USA) was 1:250, and for XRCC1 (Rabbit polyclonal, ab58465; Abcam) was diluted at 1:500. The membranes were washed with TBST three times for 10–15 min and incubated with HRP-conjugated rabbit secondary antibody (Goat anti-Rabbit IgG H + L Secondary Antibody, HRP. Prod. 31,460, Pierce Thermo Scientific, Rockford, IL, USA) at 1:10,000 dilution in 1% BSA and TBST for 1 h, under constant shaking at room temperature. Then, the membranes were washed with TBST five times for 10 min under constant shaking at room temperature for detection of target protein by chemiluminescence. The same membranes were stripped for reprobing of housekeeping protein used as loading control for quantification. The membranes were incubated in stripping buffer, pH 2.2 (0.2 mM glycine, 3.47 mM SDS and 1% *v*/*v* Tween 20) for 5 min, twice, and then were washed in PBS twice for 10 min and in TBST, twice for 5 min. The membrane was blocked with 2.5% non-fat dry milk for 1 h at room temperature. The incubation with housekeeping antibody was performed at 4 °C overnight. The dilution used for β-actin (beta actin loading control anti-mouse monoclonal antibody BA3R, MA515739, Thermo Fisher Scientific, Rockford, IL, USA) was 1:2500. For reprobing α-tubulin (alpha tubulin monoclonal antibody DM1A, 62204, Thermo Fisher Scientific, Rockford, IL, USA), the dilution was 1:5000. Thereafter, the membranes were washed with TBST three times for 15 min and incubated with HRP-conjugated rabbit secondary antibody (Goat anti-Mouse IgG (H + L) Secondary Antibody, HRP. Prod: 31430; Pierce Thermo Scientific, Rockford, IL, USA) at 1:10,000 dilution in 1% BSA and TBST for 1 h, under constant shaking at room temperature. Then, the membranes were washed with TBST five times for 10 min under constant shaking at RT for detection of *β-actin* or α-tubulin by chemiluminescence.

Detection, Image Acquisition, and Densitometry

For visualization of target protein detected by Western blots, the membranes were incubated in an enhanced chemiluminescence solution prepared according to the manufacturer's instructions (Perkin Elmer Life Sciences, Boston, MA). Chemiluminescence was captured by a ChemiScope 3400 (ClinX Sciences Instruments Co, Ltd. Shanghai, China), and images were digitalized and processed by ImageJ software (National Institutes of Health, USA). The background was subtracted using a rolling ball algorithm. The image for quantification was chosen within the linear range of time exposition; the measurement area was obtained as signal for each protein band. The area values were normalized by the Sum of all Data Points in replicated (Degasperi et al. 2014). Two loading controls were used for determination of normalized target protein levels (Taylor and Posch 2014) corresponding to total protein (Ponceau staining), using β-actin or α-tubulin as housekeeping. The values obtained from two loading controls were analyzed for statistical analysis. The normalized target protein levels are in arbitrary units (a.u.), as the means from the two loading controls (total protein and housekeeping).

Statistical Analysis

All results are expressed as means ± standard error of the means (SEM). Effects were evaluated by unbalanced two-way F-ANOVA, followed by Benjamini-Hochberg correction

as a post hoc test for multiple comparisons. For statistically significant differences, the probability of error was set up to less than 5%. Data analysis was performed with a XLSTAT software, version 2018. 20.1.49878 (ADDINSOFT SARL, Paris, France).

Results

Global Perinatal Asphyxia

PA was performed by immersing cesarean-removed fetuses-containing uterine horns from *on-term* rat dams into a water bath at 37 °C for 21 min, using sibling cesarean-delivered fetuses for comparisons. The rate of survival shown by AS neonates was approximately 60%, while it was 100% for control (CS) neonates. Surviving AS neonates showed decreased respiratory frequency supported by gasping, decreased vocalization, cyanotic skin, rigidity, and akinesia, indicating a severe metabolic insult. Asphyxia-exposed and control neonates were, however, nurtured well by surrogate dams up to postnatal (P) day P1 or P14, when they were euthanized for dissecting samples from hippocampus to be assayed for glutathione, GR, GPx, catalase, TIGAR, calpain, and XRCC1. A series of asphyxia-exposed and control neonates was injected with either 100 μl saline or 0.8 mmol/kg of nicotinamide, i.p., 1 h after delivery.

Effect of Perinatal Asphyxia and Nicotinamide on Hippocampus Glutathione (GSH, GSSG, and GSSG/GSH Ratio) Levels

The effect of PA on GSH and GSSG levels and GSSG/GSH ratio evaluated in hippocampus from CS and AS rat neonates at P1 and 14 is summarized in section A of Table 1. PA increased GSSG (~2-fold) levels at P1 and P14. GSH levels were decreased by 36%, but only at P14. The GSSG/GSH ratio was calculated for each individual, as an index of oxidative stress (Németh and Boda 1989). Unbalanced two-way F-ANOVA indicated a significant effect of PA and postnatal days on GSSG/GSH ratio, increased ~2-fold at P1 and >4-fold at P14, compared to that observed in CS neonates at the same age.

The effect of neonatal nicotinamide treatment is summarized in section B of Table 1, showing that GSH levels were increased (~2-fold), both in control and asphyxia-exposed neonates. The GSSG/GSH ratio decreased in all cases, at P1 and P14. Nicotinamide treatment also decreased GSSG levels, but only in asphyxia-exposed animals.

Effect of Perinatal Asphyxia and Nicotinamide on Hippocampus GR and GPx Activity

As shown in section A of Table 2, PA produced a decrease in GR and GPx enzymatic activity at P1 and P14. Section B of Table 2 shows the effect of nicotinamide that increased GR enzymatic activity in control neonates at P1 and P14, while GPx activity was only increased at P14. In asphyxia-exposed neonates, nicotinamide increased the enzymatic activity of both GR and GPX, at P1 and P14.

Effect of Perinatal Asphyxia and Nicotinamide on Hippocampus Catalase Activity (Fig. 1)

Fig. 1 shows representative immunoblots of the effect of PA and nicotinamide on catalase protein in hippocampus of rat neonates at P1 (a) and at P14 (b). Table 3 summarizes the effect of PA on catalase protein levels (expressed as arbitrary units, a.u.). Catalase activity was calculated for each individual, determining the *k* value for the decomposition of hydrogen peroxide, normalized by catalase relative levels and total protein. Unbalanced two-way F-ANOVA indicated a significant effect of PA and postnatal days on catalase activity in hippocampus, decreased when compared to that shown by the controls along postnatal days. A maximum effect was observed at P14, when catalase activity decreased by ~70% in AS, compared to the corresponding CS neonates (section A of Table 3).

Section B of Table 3 shows the effect of neonatal nicotinamide, which increased catalase activity at P1 (>2-fold), but not at P14 in hippocampus of CS animals. In asphyxia-exposed rat neonates, nicotinamide increased catalase levels (measured by WB and ELISA), and catalase activity at P1 and P14, with a maximum effect observed at P14 (>5-fold).

Effect of Perinatal Asphyxia and Nicotinamide on Hippocampus PPP by Monitoring TIGAR Expression (Fig. 2)

Fig. 2 shows representative immunoblots of the effect of PA and nicotinamide on TIGAR protein in hippocampus of rat neonates at P1(a) and at P14 (b). Section A of Table 4 shows the effect of PA on TIGAR levels at P1 and P14. TIGAR levels were decreased in hippocampus of asphyxia-exposed neonates at P1 but were increased at P14, compared with the controls, an effect that was prevented by nicotinamide (section B of Table 4). Nicotinamide also produced a slight but significant decrease of TIGAR levels in hippocampus of control neonates at P14.

Table 1 (a) Effect of perinatal asphyxia (PA) and (b) nicotinamide (0.8 mmol/kg, i.p.) or vehicle (0.1 ml NaCl 0.9%, i.p.) on glutathione (GSSG, GSH; μmol/mg) levels and GSSG/GSH ratio monitored in hippocampus of rat neonates at P1 and P14. (Comparisons: AS versus CS; CS nicotinamide versus CS vehicle; AS nicotinamide versus AS vehicle)

Animals	GSH (μmol/mg)	GSSG (μmol/mg)	GSSG/GSH ratio	GSH (μmol/mg)	GSSG (μmol/mg)	GSSG/GSH ratio
A. Effect of PA	P1			P14		
CS	7.49 ± 0.70	0.08 ± 0.01	0.011 ± 0.0005	8.91 ± 0.30	0.07 ± 0.01	0.008 ± 0.001
n = 8						
AS	7.32 ± 0.31	*0.15 ± 0.01*	*0.02 ± 0.002*	*5.71 ± 0.59 (by*	*0.16 ± 0.01*	*0.031 ± 0.003*
n = 8–9		*(> 1.9 ± 0.15x)*****	*(> 1.9X ± 0.10)*****	*35.85 ± 6.28%)*****	*(> 2.5 ± 0.42x)*****	*(> 4.1 ± 0.72)*****
B. Effect of nicotinamide	P1			P14		
CS Vehicle	7.13 ± 0.44	0.07 ± 0.002	0.01 ± 0.0011	10.09 ± 1.01	0.08 ± 0.01	0.01 ± 0.001
n = 8–10						
CS nicotinamide	*12.11 ± 0.88*	0.08 ± 0.01	0.007 ± 0.001 *(by*	*23.06 ± 1.30*	0.08 ± 0.01	*0.004 ± 0.001 (by*
n = 9–10	*(> 1.7 ± 0.18x)*****		*32.81 ± 7.97%)**	*(> 2.4 ± 0.26x)*****		*61.76 ± 6.27%)*****
AS vehicle	7.53 ± 0.65	0.16 ± 0.01	0.02 ± 0.001	4.83 ± 0.49	0.14 ± 0.005	*0.03 ± 0.002*
n = 8–10						
AS nicotinamide	*13.70 ± 1.09*	*0.09 ± 0.01 (by*	0.007 ± 0.0003 *(by*	*11.82 ± 1.08*	*0.07 ± 0.003 (by*	*0.007 ± 0.001 (by*
n = 9–12	*(> 1.8 ± 0.23x)*****	*42.78 ± 5.72%)*****	*68.79 ± 2.51%)*****	*(> 2.8 ± 0.5x)*****	*44.04 ± 5.03%)*****	*75.26 ± 4.55%)*****

GSH and GSSG were measured by a recycling method at 412 nm and the concentration normalized by total protein. All values are means ± S.E.M., from at least $N = 4$ independent experiments in duplicated. Unbalanced two-way F-ANOVA indicated a significant effect of PA and postnatal days on GSSG/GSH ratio ($F_{(3, 29)} = 17.096$, $P < 0.0001$) and a significant effect of nicotinamide and postnatal days ($F_{(7, 69)} = 61.584$, $P < 0.0001$). Benjamini-Hochberg was used as a post hoc test

* $P < 0.05$; ** $P < 0.01$; *** $P < 0.001$; **** $P < 0.0001$ in italics

Effect of Perinatal Asphyxia and Nicotinamide on Hippocampus Calpain Activity

In section A of Table 5, the effect of PA on hippocampus calpain activity is shown at P1 and P14. There was a 2-fold increase in calpain activity in PA-exposed compared with CS animals at P14. As shown in section B of Table 5, nicotinamide did not have any effect in CS animals, but it decreased calpain activity, compared to saline-treated AS animals at P14 (by ~60%).

Effect of Perinatal Asphyxia and Nicotinamide on Hippocampus XRCC1 Levels (Fig. 3)

Fig. 3 shows representative immunoblots of the effect of PA and nicotinamide on XRCC1 protein in hippocampus of rat neonates at P1 (a) and at P14 (b). As is shown in section A of Table 5, PA induced a significant but minor increase of XRCC1 protein levels, but only at P1, compared with CS animals. The effect of nicotinamide on XRCC1 protein levels is shown in section B of Table 5, decreasing the enhancement induced by PA at P1.

Discussion

The present study evaluates the effect of PA on redox regulation in rat hippocampus at P1 and P14, and evaluating also the effect of intraperitoneal administration of nicotinamide administered 1 h after delivery. It was found that global PA produced (i) a sustained increase of GSSG levels and GSSG/GSH ratio at P1 and P14; (ii) a decrease of GR, GPx, and catalase activity at P1 and P14; (iii) a decrease of TIGAR levels at P1, followed by an increase at P14; (iv) an increase of calpain activity at P14; and (v) an increase of XRCC1 levels, but only at P1. (vi) Nicotinamide prevented the effect of PA on GSSG levels and GSSG/GSH ratio, and on GR, GPx, and catalase activity, also on increased TIGAR levels and calpain activity observed at P14.

The study expands and support a previous report showing that global PA in rats induces a regionally sustained impairment in redox homeostasis, demonstrating here that oxidative stress induced by PA is further associated with decreased activity of GR, GPx, and catalase, enzymes regulating glutathione and H_2O_2 levels, respectively, and with a shift towards TIGAR-dependent PPP, and delayed cell death, reflected by an increase of calpain activity, in agreement with previous reports demonstrating that PA leads to increased cleaved caspase-3 expression (Lespay-Rebolledo et al. 2018) and apoptotic cell death (Neira-Peña et al. 2015) in hippocampus of PA-exposed rat neonates. The effect of PA on calpain activity was observed at P14, a time at which an increase in caspase-3 levels was not longer observed (Lespay-Rebolledo et al. 2018),

Table 2 (a) Effect of perinatal asphyxia (PA) and (b) nicotinamide (0.8 mmol/kg, i.p.) or vehicle (0.1 ml NaCl 0.9%, i.p.) on glutathione reductase (GR) and glutathione peroxidase (GPx) activity monitored in hippocampus of rat neonates at P1 and P14. (Comparisons: AS versus CS; CS nicotinamide versus CS vehicle; AS nicotinamide versus AS vehicle)

Animals	GR mu/mL/μg protein	GPX (NADPH nmol/mL/mg protein)	GR (mu/mL/μg protein)	GPX (NADPH nmol/mL/mg protein)
A. Effect of PA	P1		P14	
CS	8.39 ± 0.60	786.69 ± 109.46	5.12 ± 0.33	839.31 ± 53.09
$n = 6–14$				
AS	*5.36 ± 0.71 (by 29.2 ± 4.58%)***	*369.80 ± 29.28 (by 51.4 ± 6.76%)***	*3.75 ± 0.28 (by 27.9 ± 6.4%)***	*385.27 ± 49.41 (by 52.72 ± 7.37%)****
N = 6–10				
B. Effect of nicotinamide	P1		P14	
CS Vehicle	7.58 ± 0.63	656.06 ± 35.16	5.91 ± 0.31	808.21 ± 76.14
$n = 6–9$				
CS nicotinamide	*13.28 ± 1.24 (> 1.7 ± 0.13x)***	772.16 ± 36.90	*7.89 ± 0.57 (> 1.3 ± 0.09x)**	*1764.97 ± 138.44 (> 2.3 ± 0.31x)****
$n = 10–16$				
AS vehicle	4.54 ± 0.39	408.88 ± 28.85	4.40 ± 0.25	459.90 ± 45.38
$n = 6–11$				
AS nicotinamide	*14.73 ± 2.09 (> 3.6 ± 0.63x)****	*904.32 ± 95.99 (> 2.3 ± 0.33x)****	*7.78 ± 0.55 (> 1.8 ± 0.15x)****	*1315.88 ± 140.71 (> 3.1x ± 0.52)****
$n = 8–10$				

GR activity is expressed as mU/ml/μg protein and GPx activity as NADPH nmol/ml/mg protein. All values are means ± S.E.M., from at least $N = 3$ independent experiments in duplicates. Unbalanced two-way F-ANOVA indicated a significant effect of PA and postnatal days on GR ($F_{(3, 40)} = 43.897$, $P < 0.0001$) and GPx ($F_{(3, 23)} = 55.633$, $P < 0.0001$). The effect of nicotinamide and postnatal days on GR ($F_{(7, 69)} = 15.810$, $P < 0.0001$) and on GPx ($F_{(7, 49)} = 37.536$, $P < 0.0001$) activity was statistically significant. Benjamini-Hochberg was used as a post hoc test

*$P < 0.05$; **$P < 0.01$; ***$P < 0.001$; ****$P < 0.0001$ in italics

suggesting a caspase-3-independent, but bax-dependent delayed cell death, as previously proposed, showing mitochondrial impairment to precede neuronal death (D'Orsi et al. 2012). An increase of XRCC1 levels was only observed at P1 after PA, in agreement with previous observations regarding PARP-1 overexpression, restricted in hippocampus to the first hours after delivery (Neira-Peña et al. 2014, 2015), prevented, however, by neonatal nicotinamide treatment (Allende-Castro et al. 2012; Neira-Peña et al. 2015) and selective siRNA PARP-1 knockdown (Vio et al. 2018). The increase in XRCC1 levels induced by PA was also prevented by nicotinamide, in agreement with the proposal that XRCC1 is involved in DNA repairing, interacting with DNA ligase III, polymerase β, and PARP-1 (London 2015), also following PA (Chiappe-Gutierrez et al. 1998; see Herrera-Marschitz et al. 2014). Thus, the present results support the idea that brain damage continues long after the re-oxygenation period, extending to days and/or weeks after PA, implying changes in metabolism, redox homeostasis, and suppression and/or overactivation of gene expression (see Hassell et al. 2015). Apoptosis in hippocampus of PA-exposed animals has been observed for periods extending 1 month (Morales et al. 2010).

It has been shown that TIGAR, a fructose-2,6 bisphosphatase, is rapidly upregulated in neurons following postnatal ischemia-reperfusion (Li et al. 2014), letting the glucose metabolism enter into the PPP (Ros and Schulze 2013; Li et al. 2014), enhancing its flux, generating NADPH, reducing GSSG to GSH, and decreasing ROS levels (Fico et al. 2004; Bensaad et al. 2006). The shunt of glucose-6-phosphate to PPP occurs by the fructose-2, 6-bisphosphatase activity of TIGAR, decreasing fructose-2, 6-biphosphate levels, inhibiting the activity of phosphofructokinase 1 (PFK1), a rate-limiting enzyme of glycolysis (Bensaad et al. 2006; Okar et al. 2001; Li et al. 2014). Also, TIGAR can relocalize to the outer mitochondrial membrane, increasing the activity of hexokinase 2 (HK2), to maintain mitochondrial membrane potential, reducing ROS levels, to prevent caspase-depending apoptosis (Cheung et al. 2012; da-Silva et al. 2004). In postnatal models of brain ischemia, TIGAR is upregulated, reaching a peak at 3 h post reperfusion, declining thereafter towards basal levels (Li et al. 2014; Cao et al. 2015). In the present study, it was found that TIGAR levels were decreased in hippocampus from AS animals at P1 but increased at P14. The decrease of TIGAR levels observed at P1 occurred together with a decrease of GR, GPx, and catalase activity, at a time when the GSSG/GSH ratio was increased ~ 2-fold. At P14, however, TIGAR levels were increased in PA-exposed animals, when the GSSG/GSH ratio was increased > 4-fold in AS compared with CS animals, while GPx and catalase activity was remarkably decreased (by more than 50%). The downregulation of TIGAR observed at P1 suggests a failure of the cell system to shunt glucose-6-phosphate to the PPP for producing NADPH during the postnatal period,

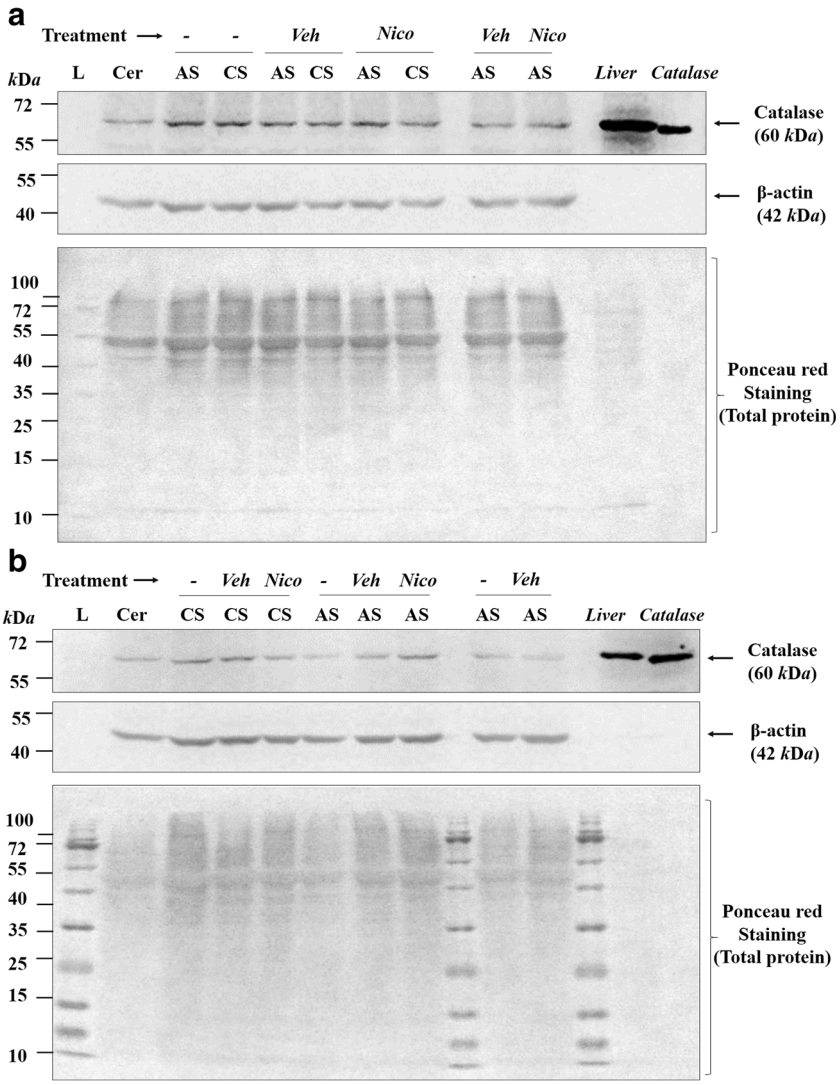

Fig. 1 Representative immunoblot of the effect of perinatal asphyxia and nicotinamide on catalase protein in hippocampus of neonatal brain rats at P1 (**a**) and P14 (**b**). The effect of perinatal asphyxia (PA) was analyzed in protein extracts from tissue sampled at P1 and 14. Control (CS) and asphyxia-exposed (AS) samples taken from sibling neonatal rats, 1 h after birth pups received an intraperitoneal injection of nicotinamide (Nico; 0.8 mmol/kg, i.p.) or NaCl 0.9% (Veh; 0.1 ml i.p.). Representative immunoblots for catalase and loading controls, corresponding to β-actin and Ponceau red staining, are shown. Catalase was identified as a unique band at 60 kDa. Extracted protein from a liver sample taken at P1 and purified catalase protein were used as positive controls. Lane Cer is an internal control from cerebellum, used to control variations in transference. Lane L corresponds to a ladder protein marker.

probably because of a reduced glutathione reductase activity (Margis et al. 2008), also observed in models of postnatal brain hypoxia/ischemia (Cao et al. 2017), reducing PPP in brain from unilaterally clamped carotid arteries, correlating with a reduction of glutathione reductase activity, 2 h after the insult (Brekke et al. 2014). The increase of TIGAR expression observed at P14, together with a reduction of GR activity, suggests a compensatory delayed mechanism, increasing PPP. However, NADPH levels resulting from this pathway did not appear to enhance the activity of NADPH-dependent enzymes, since the oxidative stress was sustained, evidenced by a high GSSG/GSH ratio still observed at P14. These results suggest that NADPH produced by PPP in AS animals is used to generate instead superoxide anion by the action of NADPH oxidase, because there is in vitro (Lu et al. 2012; Kleikers et al. 2012; Gupte et al. 2006; Balteau et al. 2011) and in vivo (Cao et al. 2017) evidence, indicating that superoxide anion production is dependent upon glucose metabolism, via the hexose monophosphate shunt to generate NADPH after ischemia-reperfusion (Suh et al. 2008; Kuehne et al. 2015). A low NADPH availability and a decreased GR activity observed at P1 and P14 after PA can explain the GSSG accumulation observed in hippocampus from AS animals up to P14, indicating that PA impairs the GR-dependent salvage pathway for GSH recycling. The salvage pathway reduces GSSG to GSH, maintaining the GSH-dependent activity of antioxidant enzymes (Lushchak 2012). The changes observed in GSH levels (by ~36% in AS animals at P14) can imply a failure of de novo synthesis of GSH, associated to metabolic deregulation of cysteine, glycine, and/or glutamate, precursors of GSH synthesis by astrocytes (Hertz and Zielke 2004).

Another issue addressed by the present study was to evaluate whether the enzymatic activity of GPx is affected by PA, since a reduced catalase activity was reported in AS animals, suggesting H_2O_2 accumulation following hypoxia and re-oxygenation (Lespay-Rebolledo et al. 2018), in agreement with a cooperative function shown between both enzymes under oxidative stress conditions (Baud et al. 2004). The present results show

Table 3 (a) Effect of perinatal asphyxia (PA) and (b) nicotinamide (0.8 mmol/kg, i.p.) or vehicle (0.1 ml NaCl 0.9%, i.p.) on catalase protein levels and activity monitored in hippocampus of rat neonates at P1 and P14. (Comparisons: AS versus CS; CS nicotinamide versus CS vehicle; AS nicotinamide versus AS vehicle)

Animals	Catalase WB (a.u.)	Catalase ELISA (absorbance/mg protein)	Catalase activity (k/catalase/mg protein)	Catalase WB (a.u.)	Catalase ELISA (absorbance/mg protein)	Catalase activity (k/catalase/mg protein)
A. Effect of PA	P1			P14		
CS $n = 4–5$	0.94 ± 0.10	0.368 ± 0.099	0.150 ± 0.022	1.074 ± 0.052	0.176 ± 0.018	0.017 ± 0.003
AS $n = 4–5$	1.04 ± 0.08	0.206 ± 0.034 *(by 36.31 ± 16.01%)***	*0.053 ± 0.009 (by 64.46 ± 5.33%)****	0.966 ± 0.054	0.105 ± 0.016 *(by 41.73 ± 7.59%)**	*0.004 ± 0.0003 (by 71.23 ± 8.33%)****
B. Effect of nicotinamide	P1			P14		
CS vehicle $n = 4–5$	0.98 ± 0.07	0.212 ± 0.029	0.102 ± 0.009	1.016 ± 0.045	0.150 ± 0.012	0.011 ± 0.001
CS nicotinamide $n = 4–5$	1.19 ± 0.08	*0.363 ± 0.047 (> 1.8 ± 0.4x)***	*0.214 ± 0.020 (> 2.2 ± 0.28x)****	0.982 ± 0.080	0.124 ± 0.028	0.009 ± 0.001
AS vehicle $n = 4–5$	1.05 ± 0.07	0.168 ± 0.075	0.065 ± 0.015	0.995 ± 0.052	0.078 ± 0.004	0.005 ± 0.001
AS Nicotinamide $n = 4–5$	*1.27 ± 0.06 (> 1.2 ± 0.08x)**	*0.399 ± 0.065 (> 3.8 ± 1.44x)***	*0.145 ± 0.015 (> 2.5 ±0.87x)****	*1.35 ± 0.076 (> 1.3 ± 0.11x)***	*0.145 ± 0.021 (> 1.8 ± 0.28x)***	*0.023 ± 0.007 (> 5.8 ± 2.27x)***

Normalized catalase protein by western blot ($N = 5$ independent experiments) is expressed in arbitrary units (a.u.), relative catalase levels by ELISA is expressed in absorbance values by total protein (mg) and catalase activity by ELISA is expressed as constant (k) rate from the exponential decomposition of hydrogen peroxide (min), normalized by catalase relative levels and total protein in milligram (mg). Data are means ± S.E.M from $N = 3$ independent experiments. Unbalanced two-way F-ANOVA indicated a significant effect of PA and postnatal days on catalase activity ($F_{(3, 13)} = 22{,}186$ $P < 0.0001$). The effect of nicotinamide and postnatal days reached the statistically significant level ($F_{(7, 29)} = 7833$ $P < 0.0001$). Benjamini-Hochberg was used as a post hoc test

*$P < 0.05$; **$P < 0.01$; ***$P < 0.001$, ****$P < 0.0001$ in italics

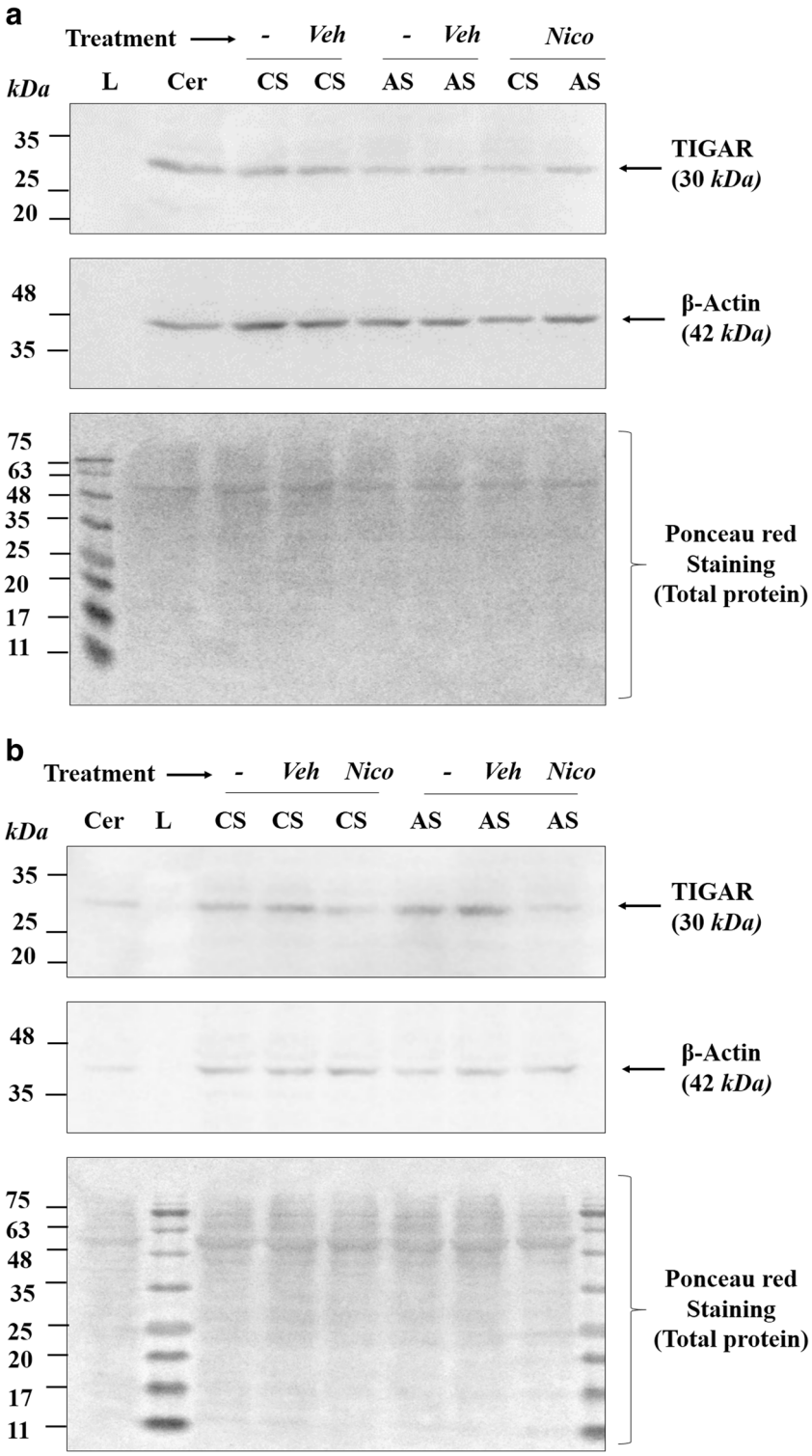

Fig. 2 Representative immunoblot of the effect of perinatal asphyxia and nicotinamide on TIGAR protein in hippocampus of neonatal brain rats at P1 (**a**) and P14 (**b**). The effect of perinatal asphyxia (PA) and nicotinamide treatment was analyzed in protein extracts from tissue sampled at P1 and P14. Control (CS) and asphyxia-exposed (AS) samples taken from sibling neonatal rats. One hour after birth, pups received an intraperitoneal injection of nicotinamide (Nico; 0.8 mmol/kg, i.p.) or 0.9% NaCl (Veh; 0.1 ml i.p.). Representative immunoblots for TIGAR and loading controls, corresponding to β-actin and Ponceau red staining. TIGAR was identified as a unique band at 30 kDa. Lane Cer is an internal control from cerebellum used to control variations in transference. Lane L corresponds to a ladder protein marker.

a decrease of around 50% in GPx activity, together with more than 60% decrease of catalase activity in AS animals at P14. GPx is the enzyme removing hydro- and lipid-peroxides, performed by two steps: (i) an oxidative reaction by which H_2O_2 binds to the catalytic site of GR, reduced to H_2O by GSH, and (ii) a reductive reaction, by which the GSSG formed in the first step is reduced to GSH. Although the second step yields is dependent of GSH, the catalytic activity of GPx this enzyme depends on the H_2O_2 concentration (Deponte 2013), while both GPx and catalase cooperatively act to remove H_2O_2 (Baud et al.

Table 4 (a) Effect of perinatal asphyxia (PA) and (b) nicotinamide (0.8 mmol/kg, i.p.) or vehicle (0.1 ml NaCl 0.9%, i.p.) on TIGAR protein levels monitored in hippocampus of rat neonates at P1 and P14. (Comparisons: AS versus CS; CS nicotinamide versus CS vehicle; AS nicotinamide versus AS vehicle)

Animals	TIGAR WB (a.u.)	TIGAR WB (a.u.)
A. Effect of PA	P1	P14
CS $n = 5$	1.38 ± 0.15	0.92 ± 0.04
AS $n = 5$	*0.80 ± 0.08 (by 35.9% ± 8.27)***	*1.29 ± 0.14 (> 1.4X ± 0.19)***
B. Effect of nicotinamide	P1	P14
CS vehicle $n = 5$	1.18 ± 0.07	0.95 ± 0.05
CS nicotinamide $n = 5$	0.95 ± 0.07	*0.71 ± 0.07 (by 28.1 ± 6.8%)***
AS vehicle $n = 5$	0.94 ± 0.09	1.44 ± 0.15
AS nicotinamide $n = 5$	0.88 ± 0.08	*0.82 ± 0.10 (by 40.7 ± 8.27%)***

TIGAR normalized levels are expressed in arbitrary units (a.u.). Data are means ± S.E.M. from $N = 5$ independent experiments. Two-way F-ANOVA indicated a significant effect of PA and postnatal days on TIGAR levels ($F_{(3, 37)} = 50.557$, $P < 0.0001$). The effect of nicotinamide and postnatal days reached the statistically significant level ($F_{(7, 73)} = 56, 911$, $P < 0.0001$). Benjamini-Hochberg was used as a post hoc test

*$P < 0.05$; **$P < 0.01$; ***$P < 0.001$, ****$P < 0.0001$ in italics

2004; Lardinois et al. 1996). At high concentrations of H_2O_2 (> 100 μM), catalase is auto-inactivated by irreversible inhibition, prevented by GPx, removing H_2O_2, to be maintained at low levels (> 1 μM), allowing the functioning of catalase (Baud et al. 2004). Therefore, the decreased GPx activity observed under AS conditions suggests that this is a consequence of high accumulation of catalase-regulated H_2O_2 (Rosenblat and Aviram 1998; see Lubos et al. 2011). High GSH levels can activate catalase, as shown by studies carried out with astrocytes, demonstrating that GSH deprivation induces auto-inactivation of catalase (Dringen and Hamprecht 1997, Sokolova et al. 2001). However, as also shown in a previous study (Lespay-Rebolledo et al. 2018), PA induced a decrease of GSH levels at P14, suggesting that at early stages following PA, a decrease of catalase activity is not a consequence of low GSH levels, but of other mechanisms increasing H_2O_2 levels, perhaps due to overactivation of SOD and/or NADPH oxidase (Kinouchi et al. 1998; Lu et al. 2012; Kleikers et al. 2012).

An important addressed issue was to evaluate the effect of nicotinamide, reversing the redox impairment induced by PA. Nicotinamide has been shown to play a fundamental role as a biological precursor for the synthesis of NAD^+ and $NADP^+$ (Kamat and Devasagayam 1999, Chong et al. 2004; Kawamura et al. 2016; Wang et al. 2016; Zhang et al. 2016), preventing oxidative stress (Turunc Bayrakdar et al. 2014). Indeed NAD^+ can be yielded by two pathways: (i) the kynurenine (from dietary tryptophan) and (ii) the salvage pathway from nicotinamide by the enzymes nicotinamide phosphoribosyl transferase and NMNAT nicotinamide deamidase (Houtkooper et al. 2010; Massudi et al. 2012; Poljsak and Milisav 2016). The synthesis of NADPH can be then driven by re-routing glycolysis to the PPP pathway (Chakrabarti et al. 2015), but also by the NAD^+ salvage pathway (Massudi et al. 2012), which via NAMPT contributes to NADPH synthesis by transference of the phosphoribosyl group from 5-phosphoribosyl-1-pyrophosphate to nicotinamide, forming nicotinamide mononucleotide (NMN), and

Table 5 (a) Effect of perinatal asphyxia (PA) and (b) nicotinamide (0.8 mmol/kg, i.p.) or vehicle (0.1 ml NaCl 0.9%, i.p.) on calpain activity and XRCC1 protein levels monitored in hippocampus of rat neonates at P1 and P14. (Comparisons: AS versus CS; CS nicotinamide versus CS vehicle; AS nicotinamide versus AS vehicle)

Animals	Calpain Units/mg total protein	XRCC1 WB (a.u)	Calpain Units/mg total protein	XRCC1 WB (a.u)
A. Effect of PA	P1		P14	
CS ($n = 5–8$)	1346.07 ± 69.07	0.88 ± 0.06	2962.24 ± 102.08	1.10 ± 0.05
AS ($n = 5–8$)	1500.19 ± 60.92	*1.14 ± 0.03 (> 1.3 ± 0.12X)***	6228.25 ± 400.74 *(> 2.05 ± 0.16X)*****	0.96 ± 0.06
B. Effect of nicotinamide	P1		P14	
CS vehicle [($n = 5–8$)]	1357.35 ± 45.57	1.01 ± 0.07	2783.57 ± 160.74	1.19 ± 0.11
CS nicotinamide [($n = 5–8$)]	1313.15 ± 51.36	0.93 ± 0.03	2627.08 ± 204.60	0.94 ± 0.10
AS vehicle [($n = 4–5$)]	1478.33 ± 53.41	1.16 ± 0.06	5972.28 ± 463.16	0.93 ± 0.06
AS nicotinamide[($n = 5–8$)]	1597.31 ± 115.82	*0.81 ± 0.06 (by 29.34 ± 6.86%)****	2247.91 ± 74.04 *(by 62.40 ± 4.28%)*****	0.93 ± 0.10

Calpain activity is expressed in units/mg protein. Data are means ± S.E.M. from $N = 4$ independent experiments in duplicated. Unbalanced two-way ANOVA indicated a significant effect of PA and postnatal days on calpain activity ($F_{(3, 27)} = 111.989$, $P < 0.0001$). The effect of nicotinamide and postnatal days reached the statistically significant level ($F_{(7, 52)} = 56.117$, $P < 0.0001$). The XRCC1 protein levels are represented as protein normalized levels in arbitrary units (a.u.). Data are means ± S.E.M. from $N = 5$ independent experiments. Two-way F-ANOVA indicated a significant effect of PA and postnatal days on XRCC1 ($F_{(3, 31)} = 21.033$, $P < 0.0001$) levels. The effect of nicotinamide and postnatal days reached the statistically significant level ($F_{(7, 65)} = 69.192$, $P < 0.0001$), in italics

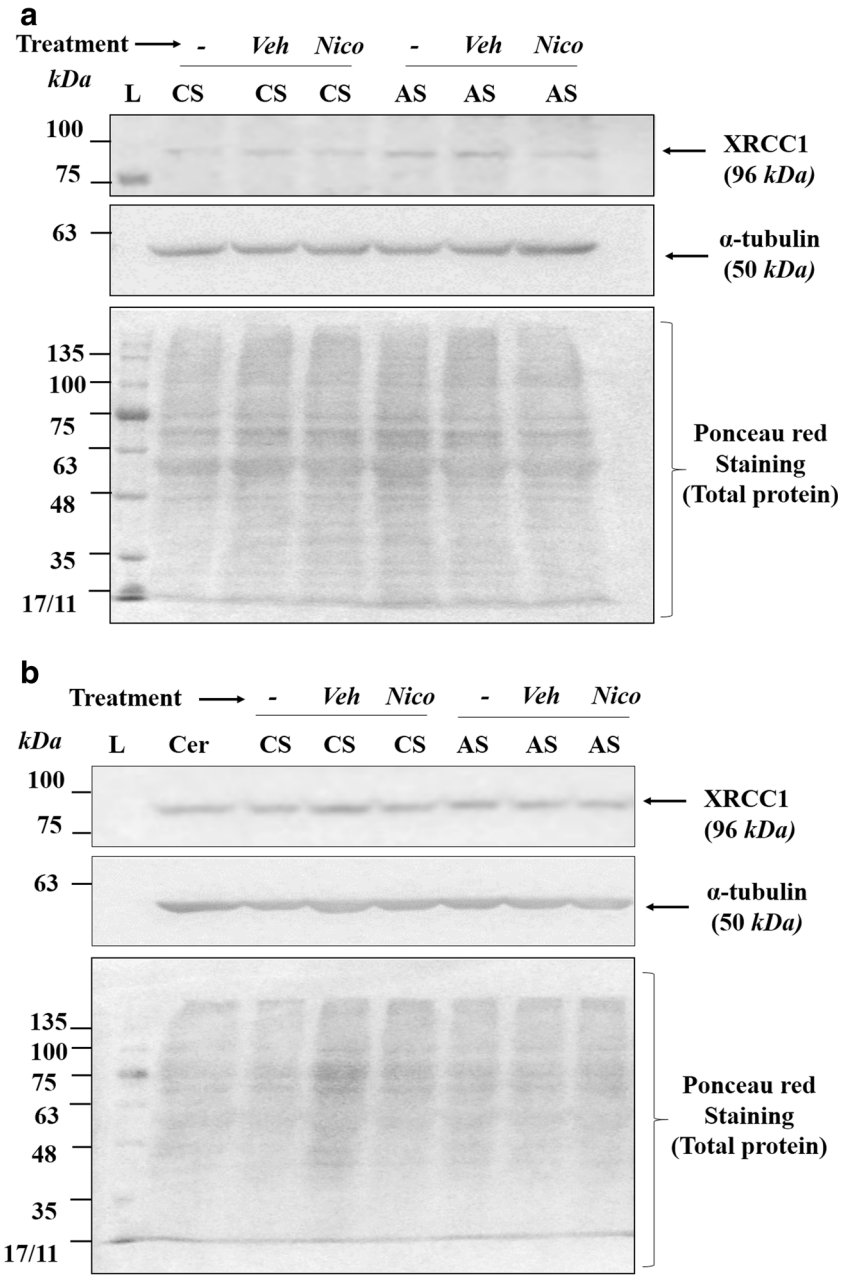

Fig. 3 Representative immunoblot of the effect of perinatal asphyxia and nicotinamide on XRCC1 protein in hippocampus of neonatal brain rats at P1 (**a**) and P14.The effect of perinatal asphyxia (PA) and nicotinamide treatment on XRCC1 was analyzed in protein extracts from tissue sampled at P1 and 14. Control (CS) and asphyxia-exposed (AS) samples taken from sibling neonatal rats. One hour after birth, pups received an intraperitoneal injection of nicotinamide (Nico; 0.8 mmol/kg, i.p.) or NaCl 0.9% (Veh; 0.1 ml i.p.). Representative immunoblots of XRCC1 and loading controls, corresponding to α-tubulin and Ponceau red staining, are shown. XRCC1 was identified as a unique band at 96 kDa. Lane Cer is an internal control from cerebellum used to control variations in transference. Lane L corresponds to a ladder protein marker.

pyrophosphate. The coupling with NAD^+ kinase (NADK) to generate $NADP^+$ from NAD^+ contributes to NADPH synthesis (Massudi et al. 2012). Thus, nicotinamide administration probably contributes to restore the redox homeostasis under a sustained oxidative stress induced by PA, increasing $NADP^+$, acting on the NAD^+ salvage pathway. It was previously shown that a single injection of nicotinamide (0.8 mmol/kg, i.p.) yields cerebral nicotinamide concentration above the 10 μM range, lasting for longer than 5 h (Allende-Castro et al. 2012).

It was found here that nicotinamide enhanced the GR/NADPH and GPx/GSH antioxidant-dependent responses. The effect of nicotinamide on the PPP was only observed at P14, since TIGAR expression was downregulated by nicotinamide (by approximately 40%) in AS animals, also showing increased GR activity (2-fold) at P14, suggesting a reversion of the PPP flux to basal levels. However, at P1, TIGAR expression was not changed by nicotinamide, while GR activity was increased in both AS (4-fold) and CS (2-fold) animals, indicating that, indeed, nicotinamide enhanced NADPH levels by increasing GR activity, probably via catalytic NADPH and GSSG-dependent mechanisms (see Shan et al. 1990). The increase produced by nicotinamide on of GR levels in AS animals at P1 and P14 led to a decrease in GSSG (by 40%) and increase in GSH levels (2–3-fold), resulting in a decreased GSSG/GSH ratio, also observed in nicotinamide-treated CS animals. The effect of nicotinamide

on GSSG/GSH ratio suggests a mechanism of de novo *synthesis*, since nicotinamide-treated CS animals showed increased GSH levels without any changes in GSSG levels (see Lubos et al. 2011).

Nicotinamide increased GPx and catalase activity in AS-treated animals at P1 and P14, a maximal effect observed at P14. Apart of allosteric mechanisms mediated by substrates and products (Ramos-Martinez 2017), post transductional modifications mediated by oxidative stress can contribute to enzyme inactivation (Miyamoto et al. 2003; Ghosh et al. 2006). Also, transcriptional modifications control cause up-regulation of expression, resulting in increased enzymatic activity (Franco-Enzástiga et al. 2017). In the present study, CS animals treated with nicotinamide showed increased GR activity at P1, compared to basal levels, suggesting that the effect of nicotinamide on enzymatic activity observed in CS and AS animals implies GR upregulation by transcriptional control (Zhu et al. 2005). At P14, the increased GR activity would be a consequence of reduction of ROS levels by nicotinamide, indicated by a decreased GSSG/GSH ratio, observed in CS and AS nicotinamide-treated animals (Dunning et al. 2013). Although, a statistical significant increase in catalase expression was observed in nicotinamide-treated CS and AS animals at P1 and P14, that slight increase had no effect on basal catalase activity, suggesting that the observed increase in enzymatic activity is due to a decrease of post transductional modifications mediated by ROS (Ghosh et al. 2006).

Finally, we investigated whether oxidative stress induced by PA can produce changes on calpain activity and XRCC1 expression, in agreement with hippocampus cell damage induced by PA. In a recent report (Lespay-Rebolledo et al. 2018), it was shown that PA induced caspase-dependent cell death at P3 and P7, but not at P1 and P14, suggesting other molecular mechanisms of cell death, as discussed above. In ischemia-reperfusion postnatal models, oxidative stress induces DNA strand breaks (SSBR), leading to polyADP ribosylation sites that accumulate XRCC1 (El-Khamisy et al. 2003; Wei et al. 2013). The downregulation of XRCC1 expression has been associated with DNA fragmentation, and apoptosis and necrosis-dependent cell death in models of brain ischemia (Fujimura et al. 1999; Ghosh et al. 2015), although it was found here that XRCC1 was upregulated at P1, perhaps as a consequence of DNA damage. A sustained oxidative damage causes depletion of NAD^+ and ATP, enhanced by PARP-1 overactivation, increasing (i) mitochondrial release of AIF and (ii) influx of calcium from extracellular and intracellular stores, activating μ-calpain that cleaves AIF, inducing translocation to the nucleus for producing DNA breakdown and cell death by necrosis (Bentle et al. 2006; Cheng et al. 2018). Depending upon Ca^{+2} levels, calpain promotes cell death or cell survival by bax-, bid-, and XIAP-mediated μ-calpain cleavage, resulting in apoptosis (Cheng et al. 2018). Also, μ-calpain can translocate to nucleus, cleaving p53 and PARP-1 and DNA III ligase, leading to nuclear condensation (Bordone and Campbell 2002). Calpain can also regulate programmed necrosis induced by TNF-α (Cheng et al. 2018).

The effect of PA on calpain activity, increased at P14, can reflect calpain 1 activation, associated with fragmentation of dendritic processes and neuronal degeneration in HI brain neonatal models (Neumar et al. 2001), showing an initial activation of calpain 1, short after the insult, decreased at 2–48 h, but again increased at P14 to P21 (Ostwald et al. 1993; Blomgren et al. 1999), leading to apoptosis-independent cell death, associated to caspase 7, 8, and 9 (Chua et al. 2000; Neumar et al. 2003). In the present study, the increased calpain activity and the effect of nicotinamide observed at P14 also indicates a role of oxidative stress on calpain activation, due to increased cytosolic Ca^{+2} levels, mitochondrial dysfunction, and endoplasmic reticulum stress (Ermak and Davies 2002), producing activation of calpain 1 (Yamada et al. 2012). Whether calpain mediates the cell damage induced by PA in hippocampus, via necrosis or programmed necrosis, is something that requires further investigation, including evaluation of the role of AIF release and/or TNF-α signaling, as shown by Neira-Peña et al. (2015) and Cheng et al. (2018).

In conclusion, the sustained oxidative stress induced by PA causes in hippocampus a reduced antioxidant response, leading to an increase of GSSG/GSH ratio in parallel with decreased GR, GPX, and catalase activity, at P1 and P14. PA triggers activation of survival pathways, to reduce oxidative stress, increasing NADPH, TIGAR, and XRCC1 availability, changing PPP flux and DNA repair, attenuating, perhaps, but not avoiding the effect of severe PA on cell death observed in hippocampus at P14, associated with increased calpain activity, indicating a caspase-independent mechanism for delayed cell death. Nicotinamide, as a $NAD^+/NADP^+$ precursor, increased the activity of antioxidant enzymes, restoring GSH, decreasing cell death in hippocampus. These effects, mediated by nicotinamide, suggest a metabolic modulation towards restoring redox homeostasis, which can play a fundamental therapeutical role to prevent the progression of brain damage and the long-term neurological deficits affecting neonates surviving PA.

Acknowledgements Contract grant sponsors: FONDECYT-Chile (no. 1120079, MHM; 1180042, YI, PMR, MHM; 1190562, PMR). CONICYT Operational Support no. 21140281 (LRC) and no. 21151232 (TBA). CONICYT-Chile fellowships: no. 21140281 (LRC) and no. 21151232 (TBA).

Compliance with ethical standards

Ethic statement All procedures were conducted in accordance with the animal care and use protocol established by a Local Ethics Committee for experimentation with laboratory animals at the Medical Faculty, University of Chile (Protocol CBA no. 0722 FMUCH) and by an ad hoc commission of the Chilean Council for Science and Technology Research (CONICYT), endorsing the principles of laboratory animal care

(NIH; No. 86-23; revised 1985). Animals were permanently monitored (on 24 h basis) regarding well being, following the ARRIVE guidelines for reporting animal studies (www.nc3rs.org.uk/ARRIVE).

References

Ahearne CE, Boylan GB, Murray DM (2016) Short and long term prognosis in perinatal asphyxia: an update. World J Clin Pediatr 5(1):67–74. https://doi.org/10.5409/wjcp.v5.i1.67

Allende-Castro C, Espina-Marchant P, Bustamante D, Rojas-Mancilla E, Neira T, Gutierrez-Hernandez MA, Esmar D, Valdes JL, Morales P, Gebicke-Haerter PJ, Herrera-Marschitz M (2012) Further studies on the hypothesis of PARP-1 inhibition as strategy for lessening the long-term effects produced by perinatal asphyxia: effects of nicotinamide and theophylline on PARP-1 activity in brain and peripheral tissue. Neurotox Res 22:79–90. https://doi.org/10.1007/s12640-012-9310-2

Balteau M, Tajeddine N, de Meester C, Ginion A, Des Rosiers C, Brady NR, Sommereyns C, Horman S, Vanoverschelde JL, Gailly P, Hue L, Bertrand L, Beauloye C (2011) NADPH oxidase activation by hyperglycaemia in cardiomyocytes is independent of glucose metabolism but requires SGLT1. Cardiovasc Res 92(2):237–246. https://doi.org/10.1093/cvr/cvr230

Baud O, Greene AE, Li J, Wang H, Volpe JJ, Rosenberg PA (2004) Glutathione peroxidase-catalase cooperativity is required for resistance to hydrogen peroxide by mature rat oligodendrocytes. J Neurosci 24(7):1531–1540. https://doi.org/10.1523/JNEUROSCI.3989-03.2004

Bensaad K, Tsuruta A, Selak MA, Vidal MN, Nakano K, Bartrons R, Gottlieb E, Vousden KH (2006) TIGAR, a p53-inducible regulator of glycolysis and apoptosis. Cell. 126(1):107–120. https://doi.org/10.1016/j.cell.2006.05.036

Bentle MS, Reinicke KE, Bey EA, Spitz DR, Bootman DA (2006) Calcium dependent modulation of poly(ADP-ribose) polymerase 1 alters cellular metabolism and DNA repair. J Biol Chem 281(44):33684–33696. https://doi.org/10.1074/jbc.M603678200

Blomgren K, Hagberg H (2005) Free radicals, mitochondria, and hypoxia-ischemia in the developing brain. Brain Pathol 15(3):234–240. https://doi.org/10.1111/j.1750-3639.2005.tb00526.x

Blomgren K, Hallin U, Andersson AL, Puka-Sundvall M, Bahr BA, McRae A, Saido TC, Kawashima S, Hagberg H (1999) Calpastatin is up-regulated in response to hypoxia and is a suicide substrate to calpain after neonatal cerebral hypoxia-ischemia. J Biol Chem 274(20):14046–14052. https://doi.org/10.1074/jbc.274.20.14046

Blomgren K, Zhu C, Wang X, Karlsson JO, Leverin AL, Bahr BA, Mallard C, Hagberg H (2001) Synergistic activation of caspase-3 by m-calpain after neonatal hypoxia-ischemia: a mechanism of "pathological apoptosis"? J Biol Chem 276(13):10191–10198. https://doi.org/10.1074/jbc.M007807200

Bordone L, Campbell C (2002) DNA ligase III is degraded by calpain during cell death induced by DNA-damaging agents. J Biol Chem 277(29):26673–26680. https://doi.org/10.1074/jbc.M112037200

Brekke EM, Morken TS, Widerøe M, Håberg AK, Brubakk AM, Sonnewald U (2014) The pentose phosphate pathway and pyruvate carboxylation after neonatal hypoxic-ischemic brain injury. J Cereb Blood Flow Metab 34(4):724–734. https://doi.org/10.1038/jcbfm.2014.8

Cao L, Chen J, Li M, Qin YY, Sun M, Sheng R, Han F, Wang G, Qin ZH (2015) Endogenous level of TIGAR in brain is associated with vulnerability of neurons to ischemic injury. Neurosci Bull 31(5):527–540. https://doi.org/10.1007/s12264-015-1538-4

Cao L, Zhang D, Chen J, Qin YY, Sheng R, Feng X, Chen Z, Ding Y, Li M, , Qin ZH (2017) G6PD plays a neuroprotective role in brain ischemia through promoting pentose phosphate pathway. Free Radic Biol Med 112: 433–444. https://doi.org/10.1016/j.freeradbiomed.2017.08.011

Chakrabarti G, Gerber DE, Boothman DA (2015) Expanding antitumor therapeutic windows by targeting cancer-specific nicotinamide adenine dinucleotide phosphate-biogenesis pathways. Clin Pharm 7:57–68. https://doi.org/10.2147/CPAA.S79760

Cheng SY, Wang SC, Lei M, Wang Z, Xiong K (2018) Regulatory role of calpain in neuronal death. Neural Regen Res 13(3):556–562. https://doi.org/10.4103/1673-5374.228762

Cheung EC, Ludwig RL, Vousden KH (2012) Mitochondrial localization of TIGAR under hypoxia stimulates HK2 and lowers ROS and cell death. Proc Natl Acad Sci U S A 109(50):20491–20496. https://doi.org/10.1073/pnas.1206530109

Chiappe-Gutierrez M, Kitzmueller E, Labudova O, Fuerst G, Hoeger H, Hardmeier R, Nohl H, Gille L, Lubec B (1998) mRNA levels of the hypoxia inducible factor (HIF-1) and DNA repair genes in perinatal asphyxia of the rat. Life Sci 63(13):1157–1167. https://doi.org/10.1016/S0024-3205(98)00377-4

Chong ZZ, Lin SH, Maiese K (2004) The NAD+ precursor nicotinamide governs neuronal survival during oxidative stress through protein kinase B coupled to FOXO3a and mitochondrial membrane potential. J Cereb Blood Flow Metab 24(7):728–743. https://doi.org/10.1097/01.WCB.0000122746.72175.0E

Chua BT, Guo K, Li P (2000) Direct cleavage by the calcium-activated protease calpain can lead to inactivation of caspases. J Biol Chem 275(7):5131–5135. https://doi.org/10.1074/jbc.275.7.5131

da-Silva WS, Gómez-Puyou A, de Gómez-Puyou MT, Moreno-Sanchez R, De Felice FG, de Meis L, Oliveira MF, Galina A (2004) Mitochondrial bound hexokinase activity as a preventive antioxidant defense: steady-state ADP formation as a regulatory mechanism of membrane potential and reactive oxygen species generation in mitochondria. J Biol Chem 279(38):39846–39855. https://doi.org/10.1074/jbc.M403835200

Degasperi A, Birtwistle MR, Volinsky N, Rauch J, Kolch W, Kholodenko BN (2014) Evaluating strategies to normalise biological replicates of Western blot data. PLoS One 9(1):e87293

Dell'Anna E, Chen Y, Engidawork E, Andersson K, Lubec G, Luthman J, Herrera-Marschitz M (1997) Delayed neuronal death following perinatal asphyxia in rat. Exp Brain Res 115:105–115. https://doi.org/10.1007/PL00005670

Deponte M (2013) Glutathione catalysis and the reaction mechanisms of glutathione-dependent enzymes. Biochim Biophys Acta 1830(5):3217–3266. https://doi.org/10.1016/j.bbagen.2012.09.018

D'Orsi B, Bonner H, Tuffy LP, Düssmann H, Woods I, Courtney MJ, Ward MW, Prehn JH (2012) Calpains are downstream effectors of bax-dependent excitotoxic apoptosis. J Neurosci 32(5):1847–1858. https://doi.org/10.1523/JNEUROSCI.2345-11.2012

Dringen R (2000) Metabolism and functions of glutathione in brain. ProgNeurobiol. 62(6):649–671. https://doi.org/10.1016/S0301-0082(99)00060-X

Dringen R, Hamprecht B (1997) Involvement of glutathione peroxidase and catalase in the disposal of exogenous hydrogen peroxide by cultured astroglial cells. Brain Res 759(1):67–75. https://doi.org/10.1016/S0006-8993(97)00233-3

Dunning S, Ur Rehman A, Tiebosch MH, Hannivoort RA, Haijer FW, Woudenberg J, van den Heuvel FA, Buist-Homan M, Faber KN, Moshage H (2013) Glutathione and antioxidant enzymes serve complementary roles in protecting activated hepatic stellate cells against hydrogen peroxide-induced cell death. Biochim Biophys Acta 1832:2027–2034. https://doi.org/10.1016/j.bbadis.2013.07.008

El-Khamisy SF, Masutani M, Suzuki H, Caldecott KW (2003) A requirement for PARP-1 for the assembly or stability of XRCC1 nuclear foci at sites of oxidative DNA damage. Nucleic Acids Res 31(19):5526–5533. https://doi.org/10.1093/nar/gkg761

Ermak G, Davies KJ (2002) Calcium and oxidative stress: from cell signaling to cell death. Mol Immunol 38:713–721. https://doi.org/10.1016/S0161-5890(01)00108-0

Fico A, Paglialunga F, Cigliano L, Abrescia P, Verde P, Martini G, Iaccarino I, Filosa S (2004) Glucose-6-phosphate dehydrogenase plays a crucial role in protection from redox-stress-induced apoptosis. Cell Death Differ 11(8):823–831. https://doi.org/10.1038/sj.cdd.4401420

Fleiss B, Gressens P (2012) Tertiary mechanisms of brain damage: a new hope for treatment of cerebral palsy? Lancet Neurol 11(6):556–566. https://doi.org/10.1016/S1474-4422(12)70058-3

Franco-Enzástiga U, Santana-Martínez RA, Silva-Islas CA, Barrera-Oviedo D, Chánez-Cárdenas ME, Maldonado PD (2017) Chronic administration of S-allylcysteine activates Nrf2 factor and enhances the activity of antioxidant enzymes in the striatum, frontal cortex and hippocampus. Neurochem Res 42:3041–3051. https://doi.org/10.1007/s11064-017-2337-2

Fujimura M, Morita-Fujimura Y, Sugawara T, Chan PH (1999) Early decrease of XRCC1, a DNA base excision repair protein, may contribute to DNA fragmentation after transient focal cerebral ischemia in mice. Stroke 30(11):2456–2463. https://doi.org/10.1161/01.STR.30.11.2456

Ghosh S, Janocha AJ, Aronica MA, Swaidani S, Comhair SA, Xu W, Zheng L, Kaveti S, Kinter M, Hazen SL, Erzurum SC (2006) Nitrotyrosine proteome survey in asthma identifies oxidative mechanism of catalase inactivation. J Immunol 176(9):5587–5597. https://doi.org/10.4049/jimmunol.176.9.5587

Ghosh S, Canugovi C, Yoon JS, Wilson DM 3rd, Croteau DL, Mattson MP, Bohr VA (2015) Partial loss of the DNA repair scaffolding protein, Xrcc1, results in increased brain damage and reduced recovery from ischemic stroke in mice. Neurobiol Aging 36(7):2319–2320. https://doi.org/10.1016/jneurobiolaging.2015.04.004

Gupte SA, Levine RJ, Gupte RS, Young ME, Lionetti V, Labinskyy V, Floyd BC, Ojaimi C, Bellomo M, Wolin MS, Recchia FA (2006) Glucose-6-phosphate dehydrogenase-derived NADPH fuels superoxide production in the failing heart. J Mol Cell Cardiol 41(2):340–349. https://doi.org/10.1016/j.yjmcc.2006.05.003

Hagberg H, David Edwards A, Groenendaal F (2016) Perinatal brain damage: the term infant. Neurobiol Dis 92(Pt A):102–112. https://doi.org/10.1016/j.nbd.2015.09.011

Hassell KJ, Ezzati M, Alonso-Alconada D, Hausenloy DJ (2015) New horizons for newborn brain prtection: enhancing endogenous neuroprotection. Arch Dis Child Fetal Neonatal 100:541–552. https://doi.org/10.1136/archdischild-2014-306284

Herrera-Marschitz M, Morales P, Leyton L, Bustamante D, Klawitter V, Espina-Marchant P, Allende C, Lisboa F, Cunich G, Jara-Cavieres A, Neira T, Gutierrez-Hernandez MA, Gonzalez-Lira V, Simola N, Schmitt A, Morelli M, Andrew Tasker R, Gebicke-Haerter PJ (2011) Perinatal asphyxia: current status and approaches towards neuroprotective strategies, with focus on sentinel proteins. Neurotox Res 19(4):603–627. https://doi.org/10.1007/s12640-010-9208-9

Herrera-Marschitz M, Neira-Pena T, Rojas-Mancilla E, Espina-Marchant P, Esmar D, Perez R, Muñoz V, Gutierrez-Hernandez M, Rivera B, Simola N, Bustamante D, Morales P, Gebicke-Haerter PJ (2014) Perinatal asphyxia: CNS development and deficits with delayed onset. Front Neurosci 8(47). https://doi.org/10.3389/fnins.2014.00047

Herrera-Marschitz M, Perez-Lobos R, Lespay-Rebolledo C, Tapia-Bustos A, Casanova-Ortiz E, Morales P, Valdes JL, Bustamante D, Cassels BK (2018) Targeting sentinel proteins and extrasynaptic glutamate receptors: a therapeutic strategy for preventing the effects elicited by perinatal asphyxia? Neurotox Res 33(2):461–473. https://doi.org/10.1007/s12640-017-9795-9

Hertz L, Zielke HR (2004) Astrocytic control of glutamatergic activity: astrocytes as stars of the show. Trends Neurosci 27(12):735–743. https://doi.org/10.1016/j.tins.2004.10.008

Houtkooper RH, Cantó C, Wanders RJ, Auwerx J (2010) The secret life of NAD^+: an old metabolite controlling new metabolic signaling pathways. Endocr Rev 31(2):194–223. https://doi.org/10.1210/er.2009-0026

Kamat JP, Devasagayam TP (1999) Nicotinamide (vitamin B3) as an effective antioxidant against oxidative damage in rat brain mitochondria. Redox Rep 4(4):179–184. https://doi.org/10.1179/135100099101534882

Kawamura T, Mori N, Shibata K (2016) β-nicotinamide mononucleotide, and anti-aging candidate compound, is retained in the body for longer than nicotinamide in rats. J Nutr Sci Vitaminol 62:272–276. https://doi.org/10.3177/jnsv.62.272

Kinouchi H, Kamii H, Mikawa S, Epstein CJ, Yoshimoto T, Chan PH (1998) Role of superoxide dismutase in ischemic brain injury: a study using SOD-1 transgenic mice. Cell Mol Neurobiol 18(6):609–620. https://doi.org/10.1023/A:1020677701368

Kleikers PW, Wingler K, Hermans JJ, Diebold I, Altenhöfer S, Radermacher KA, Janssen B, Görlach A, Schmidt HH (2012) NADPH oxidases as a source of oxidative stress and molecular target in ischemia/reperfusion injury. J Mol Med (Berl) 90(12):1391–1406. https://doi.org/10.1007/s00109-012-0963-3

Kuehne A, Emmert H, Soehle J, Winnefeld M, Fischer F, Wenck H, Gallinat S, Terstegen L, Lucius R, Hildebrand J, Zamboni N (2015) Acute activation of oxidative pentose phosphate pathway as first-line response to oxidative stress in human skin cells. Mol Cell 59(3):359–371. https://doi.org/10.1016/j.molcel.2015.06.017

Labudova O, Schuller E, Yeghiazaryan K, Kitzmueller E, Hoeger H, Lubec G, Lubec B (1999) Genes involved in the pathophysiology of perinatal asphyxia. Life Sci 64:1831–1838. https://doi.org/10.1016/S0024-3205(99)00125-3

Lardinois OM, Mestdagh MM, Rouxhet PG (1996) Reversible inhibition and irreversible inactivation of catalase in presence of hydrogen peroxide. BiochimBiophysActa. 1295(2):222–238. https://doi.org/10.1016/0167-4838(96)00043-X

Leaw B, Nair S, Lim R, Thornton C, Mallard C, Hagberg H (2017) Mitochondria, bioenergetics and excitotoxicity: new therapeutic targets in perinatal brain injury. Front Cell Neurosci 11(199). https://doi.org/10.3389/fncel.2017.00199

Lespay-Rebolledo C, Perez-Lobos R, Tapia-Bustos A, Vio V, Morales P, Herrera-Marschitz M (2018) Regionally impaired redox homeostasis in the brain of rats subjected to global perinatal asphyxia: sustained effect up to 14 postnatal days. Neurotox Res 34(3):660–676. https://doi.org/10.1007/s12640-018-9928-9

Li M, Sun M, Cao L, Gu JH, Ge J, Chen J, Han R, Qin YY, Zhou ZP, Ding Y, Qin ZH (2014) A TIGAR-regulated metabolic pathway is critical for protection of brain ischemia. J Neurosci 34(22):7458–7471. https://doi.org/10.1523/JNEUROSCI.4655-13.2014

Liu F, McCullough LD (2013) Inflammatory responses in hypoxic ischemic encephalopathy. Acta Pharmacol Sin 34(9):1121–1130. https://doi.org/10.1038/aps.2013.89

London RE (2015) The structural basis of XRCC1-mediated DNA repair. DNA Repair (Amst) 30:90–103. https://doi.org/10.1016/jdnarep.2015.02.005

Lu Q, Wainwright MS, Harris VA, Aggarwal S, Hou Y, Rau T, Poulsen DJ, Black SM (2012) Increased NADPH oxidase-derived superoxide is involved in the neuronal cell death induced by hypoxia-ischemia in neonatal hippocampal slice cultures. Free Radic Biol Med 53(5):1139–1151. https://doi.org/10.1016/j.freeradbiomed.2012.06.012

Lubec B, Labudova O, Hoeger H, Kirchner L, Lubec G (2002) Expression of transcription factors in the brain of rats with perinatal asphyxia. Biol Neonate 81:266–278. https://doi.org/10.1159/000056758

Lubos E, Loscalzo J, Handy DE (2011) Glutathione peroxidase-1 in health and disease: from molecular mechanisms to therapeutic opportunities. Antioxid Redox Signal 15:1957–1997. https://doi.org/10.1089/ars.2010.3586

Lushchak VI (2012) Glutathione homeostasis and functions: potential targets for medical interventions. J Amino Acids 2012(736837):1–26. https://doi.org/10.1155/2012/736837

Margis R, Dunand C, Teixeira FK, Margis-Pinheiro M (2008) Glutathione peroxidase family-an evolutionary overview. FEBS J 275:3959–3970. https://doi.org/10.1111/j.1742-4658.2008.06542.x

Marriott AL, Rojas-Mancilla E, Morales P, Herrera-Marschitz M, Tasker RA (2017) Models of progressive neurological dysfunction originating early in life. ProgNeurobiol 155:2–20. https://doi.org/10.1016/j.pneurobio.2015.10.001

Massudi H, Grant R, Guillemin GJ, Braidy N (2012) NAD+ metabolism and oxidative stress: the golden nucleotide on a crown of thorns. Redox Rep 17(1):28–46. https://doi.org/10.1179/1351000212Y.0000000001

Miyamoto Y, Koh YH, Park YS, Fujiwara N, Sakiyama H, Misonou Y, Ookawara T, Suzuki K, Honke K, Taniguchi N (2003) Oxidative stress caused by inactivation of glutathione peroxidase and adaptive responses. Biol Chem 384(4):567–574. https://doi.org/10.1515/BC.2003.064

Morales P, Reyes P, Klawitter V, Huaiquin P, Bustamante D, Fiedler JL, Herrera-Marschitz M (2005) Effects of perinatal asphyxia on cell proliferation and neuronal phenotype evaluated with organotypic hippocampal cultures. Neuroscience 135(2):421–431. https://doi.org/10.1016/j.neuroscience.2005.05.062

Morales P, Fiedler JL, Andres S, Berrios C, Huaiquin P, Bustamante D, Cardenas S, Parra E, Herrera-Marschitz M (2008) Plasticity of hippocampus following perinatal asphyxia: effects on postnatal apoptosis and neurogenesis. J Neurosci Res 86(12):2650–2662. https://doi.org/10.1002/jnr.21715

Morales P, Simola N, Bustamante D, Lisboa F, Fiedler J, Gebicke-Haerter P, Morelli M, Tasker RA, Herrera-Marschitz M (2010) Nicotinamide prevents the long-term effect of perinatal asphyxia on apoptosis, non-spatial working memory and anxiety in rats. Exp Brain Res 202(1):1–14. https://doi.org/10.1007/s00221-009-2103-z

Mosgoeller W, Kastner P, Fang-Kircher S, Kitzmueller E, Hoeger H, Sether P, Labudova O, Lubec G, Lubec B (2000) Brain RNA polymerase and nucleolar structure in perinatal asphyxia of the rat. ExpNeurol 161:174–182. https://doi.org/10.1006/exnr.1999.7232

Neira-Peña PE-M, Rojas-Mancilla E, Esmar D, Kraus C, Munoz V, Perez R, Rivera B, Bustamante D, Valdes JL, Hermoso M, Gebicke-Haerter P, Morales P, Herrera-Marschitz M (2014) Molecular, cellular, and behavioural effects produced by perinatal asphyxia: protection by poly (ADP-ribose) polymerase 1 (PARP-1) inhibition. In: Kostrzewa R (ed) Handbook of neurotoxicity. Springer, New York, pp 2075–2098. https://doi.org/10.1007/978-1-4614-5836-4_115

Neira-Peña T, Rojas-Mancilla E, Munoz-Vio V, Perez R, Gutierrez-Hernandez M, Bustamante D, Morales P, Hermoso MA, Gebicke-Haerter P, Herrera-Marschitz M (2015) Perinatal asphyxia leads to PARP-1 overactivity, p65 translocation, IL-1β and TNF-α overexpression, and apoptotic-like cell death in mesencephalon of neonatal rats: prevention by systemic neonatal nicotinamide administration. Neurotox Res 27(4):453–465. https://doi.org/10.1007/s12640-015-9517-0

Németh I, Boda D (1989) The ratio of oxidized/reduced glutathione as an index of oxidative stress in various experimental models of shock syndrome. Biomed Biochim Acta 48(2–3):S53–S57

Neumar RW, Meng FH, Mills AM, Xu YA, Zhang C, Welsh FA, Siman R (2001) Calpain activity in the rat brain after transient forebrain ischemia. Exp Neurol 170(1):27–35. https://doi.org/10.1006/exnr.2001.7708

Neumar RW, Xu YA, Gada H, Guttmann RP, Siman R (2003) Cross-talk between calpain and caspase proteolytic systems during neuronal apoptosis. J Biol Chem 278(16):14162–14167. https://doi.org/10.1074/jbc.M212255200

Okar DA, Manzano A, Navarro-Sabatè A, Riera L, Bartrons R, Lange AJ (2001) PFK-2/FBPase-2: maker and breaker of the essential biofactor fructose-2, 6-bisphosphate. Trends Biochem Sci 26(1):30–35. https://doi.org/10.1016/S0968-0004(00)01699-6

Ostwald K, Hagberg H, Andiné P, Karlsson JO (1993) Upregulation of calpain activity in neonatal rat brain after hypoxic-ischemia. Brain Res 630(1–2):289–294. https://doi.org/10.1016/0006-8993(93)90668-D

Poljsak B, Milisav I (2016) NAD+ as the link between oxidative stress, inflammation, caloric restriction, exercise, DNA repair, longevity, and health span. Rejuvenation Res 19(5):406–415. https://doi.org/10.1089/rej.2015.1767

Ramos-Martinez JI (2017) The regulation of the pentose phosphate pathway: remember Krebs. Arch Biochem Biophys 614:50e52. https://doi.org/10.1016/j.abb.2016.12.012–50e52

Ros S, Schulze A (2013) Balancing glycolytic flux: the role of 6-phosphofructo-2-kinase/fructose 2,6-bisphosphatases in cancer metabolism. Cancer Metab 1(1):8. https://doi.org/10.1186/2049-3002-1-8

Rosenblat M, Aviram M (1998) Macrophage glutathione content and glutathione preoxidase activity are inversely related to cell mediated oxidation of LDL: *in vitro* and *in vivo* studies. Free Radic Biol Med 24:305–307. https://doi.org/10.1016/S0891-5849(97)00231-1

Seidl R, Stoeckler-Ipsiroglu S, Rolinski B, Kohlhauser C, Herkner KR, Lubec B, Lubec G (2000) Energy metabolism in graded perinatal asphyxia of the rat. Life Sci 67:421–435. https://doi.org/10.1016/S0024-3205(00)00630-5

Shan X, Aw TY, Jones DP (1990) Glutathione-dependent protection against oxidative injury. Pharmac Ther 47:61–71. https://doi.org/10.1016/0163-7258(90)90045-4

Sokolova T, Gutterer JM, Hirrlinger J, Hamprecht B, Dringen R (2001) Catalase in astroglia-rich primary cultures from rat brain: immunocytochemical localization and inactivation during the disposal of hydrogen peroxide. Neurosci Lett 297(2):129–132. https://doi.org/10.1016/S0304-3940(00)01689-X

Stincone A, Prigione A, Cramer T, Wamelink MM, Campbell K, Cheung E, Olin-Sandoval V, Grüning NM, Krüger A, TauqeerAlam M, Keller MA, Breitenbach M, Brindle KM, Rabinowitz JD, Ralser M (2015) The return of metabolism: biochemistry and physiology of the pentose phosphate pathway. Biol Rev Camb Philos Soc 90(3):927–963. https://doi.org/10.1111/brv.12140

Suh SW, Shin BS, Ma H, Van Hoecke M, Brennan AM, Yenari MA, Swanson RA (2008) Glucose and NADPH oxidase drive neuronal superoxide formation in stroke. Ann Neurol 64(6):654–663. https://doi.org/10.1002/ana.21511

Swarte R, Lequin M, Cherian P, Zecic A, van Goudoever J, Govaert P (2009) Imaging patterns of brain injury in term-birth asphyxia. Acta Paediatr 98(3):586–592. https://doi.org/10.1111/j.1651-2227.2008.01156.x

Taylor SC, Posch A (2014) The design of a quantitative western blot experiment. Biomed Res Int 2014:361590. https://doi.org/10.1155/2014/361590

Turunc Bayrakdar E, Uyanikgil Y, Kanit L, Koylu E, Yalcin A (2014) Nicotinamide treatment reduces the levels of oxidative stress, apoptosis, and PARP-1 activity in A b (1– 42)-induced rat model of Alzheimer's disease. Free Radic Res 48(2):146–158. https://doi.org/10.3109/10715762.2013.857018

Vio V, Riveros AL, Tapia-Bustos A, Lespay-Rebolledo C, Perez-Lobos R, Muñoz L, Pismante P, Morales P, Araya E, Hassan N, Herrera-Marschitz M, Kogan MJ (2018) Gold nanorods/siRNA complex administration for knockdown of PARP-1: a potential treatment for perinatal asphyxia. Int J Nanomedicine 13:6839–6854. https://doi.org/10.2147/IJN.S175076

Wang S-N, Xu T-Y, Li W-L, Miao C-Y (2016) Targeting nicotinamide phosphoribosyltransferase as a potential therapeutic strategy to restore adult neurogenesis. CNS Neuroscience & Theraputics 22:431–439. https://doi.org/10.1111/cns.12539

Wei L, Nakajima S, Hsieh CL, Kanno S, Masutani M, Levine AS, Yasui A, Lan L (2013) Damage response of XRCC1 at sites of DNA single strand breaks is regulated by phosphorylation and ubiquitylation after degradation of poly(ADP-ribose). J Cell Sci 126(Pt 19):4414–4423. https://doi.org/10.1242/jcs.128272

Yamada KH, Kozlowski DA, Seidl SE, Lance S, Wieschhaus AJ, Sundivakkam P, Tiruppathi C, Chishti I, Herman IM, Kuchay SM, Chishti AH (2012) Targeted gene inactivation of calpain-1 suppresses cortical degeneration due to traumatic brain injury and neuronal apoptosis induced by oxidative stress. J Biol Chem 287(16): 13182–13193. https://doi.org/10.1074/jbc.M111.302612

Zhang H, Ryu D, Wu Y, Gariani K, Wang X, Luan P, D'Amico D, Ropellr ER, Lutolf MP, Aebersold R, Schoonjans K, Menzies KJ, Anwerx J (2016) NAD+ repletion improves mitochondrial and stem cell function and enhances life span in mice. Science 352:1436–1443. https://doi.org/10.1126/science.aaf2693

Zhu H, Itoh K, Yamamoto M, Zweier JL, Li Y (2005) Role of Nrf2 signaling in regulation of antioxidants and phase 2 enzymes in cardiac fibroblasts: protection against reactive oxygen and nitrogen species-induced cell injury. FEBS Lett 579(14):3029–3036